



Review

# Surface Modification of Iron Oxide-Based Magnetic Nanoparticles for Cerebral Theranostics: Application and Prospection

Yanyue Wu <sup>1,2</sup>, Zhiguo Lu <sup>1,2</sup>, Yan Li <sup>1</sup>, Jun Yang <sup>1,2,\*</sup> and Xin Zhang <sup>1,2,\*</sup>

<sup>1</sup> National Key Laboratory of Biochemical Engineering, Institute of Process Engineering, Chinese Academy of Sciences, Beijing 100190, China; yywu@ipe.ac.cn (Y.W.); zglu18@ipe.ac.cn (Z.L.); liyan310@ipe.ac.cn (Y.L.)

<sup>2</sup> School of Chemical Engineering, University of Chinese Academy of Sciences, Beijing 100049, China

\* Correspondence: jyang2012@ipe.ac.cn (J.Y.); xzhang@ipe.ac.cn (X.Z.)

Received: 1 June 2020; Accepted: 11 July 2020; Published: 24 July 2020



**Abstract:** Combining diagnosis with therapy, magnetic iron oxide nanoparticles (INOPs) act as an important vehicle for drug delivery. However, poor biocompatibility of INOPs limits their application. To improve the shortcomings, various surface modifications have been developed, including small molecules coatings, polymers coatings, lipid coatings and lipopolymer coatings. These surface modifications facilitate iron nanoparticles to cross the blood-brain-barrier, which is essential for diagnosis and treatments of brain diseases. Here we focus on the characteristics of different coated INOPs and their application in brain disease, particularly gliomas, Alzheimer's disease (AD) and Parkinson's disease (PD). Moreover, we summarize the current progress and expect to provide help for future researches.

**Keywords:** theranostics; iron oxide magnetic nanoparticles; blood-brain barrier; surface coating; target therapy

## 1. Introduction

Magnetic nanoparticles have drawn worldwide attention for their nanoscale physicochemical properties, especially in theranostics [1–8]. Combining diagnosis with therapy, magnetic nanoparticles have a pivotal role in the field of medicine [9–13]. Iron, as the most abundant organic metallic element, has emerged as the most appealing candidate [14,15]. Magnetite ( $\text{Fe}_3\text{O}_4$ ) and maghemite ( $\gamma\text{-Fe}_2\text{O}_3$ ) in particular, display size-control superparamagnetism, and are used in magnetic resonance imaging (MRI). There have been two generations of iron contrast agents (CAs) for MRI, the first one has diagnostic capability only while the new one, combining diagnosis with therapy, has multiple functions. The new one loaded with therapeutic agents after surface coating to facilitate MRI guided drug delivery, gene delivery, photothermal therapy (PTT), photodynamic therapy (PDT) or magnetic hyperthermia has gained attention [16] (Figure 1). By grafting biorecognition molecules (ligands) onto the surface of nanoparticles, active targeted therapy expands the application of new-generation CAs [17,18].

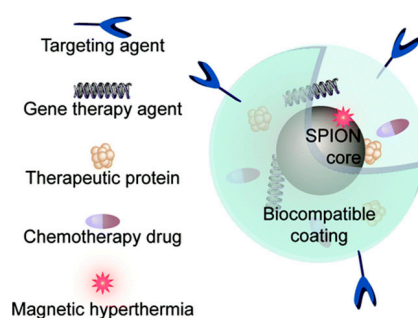


**Figure 1.** Architecture of second-generation iron-based nano-theranostics. Reproduced from “Surface Engineering of Iron Oxide Nanoparticles for Targeted Cancer Therapy”, with permission from American Chemical Society, 2011.

As a protective barrier for the central nervous system, the blood-brain barrier (BBB) limits uptake of drugs in brain cells [19,20]. Because of the tight cell junction, low efficiency of endocytosis, expression of outwardly drug efflux transporters, and high level of drug-metabolizing enzymes of BBB [21], it is difficult for drugs to pass through BBB. Ligand-based active targeted therapy opens a new way to improve the effect of drug treatment [22]. Many researches have taken up ligand-targeted surface-modified iron nanoparticles (INOPs) in brain diseases. Here the review summarizes the application of INOPs in cerebral theranostics, particularly in glioblastoma multiforme (GBM), Alzheimer’s Disease and Parkinson’s disease.

### 1.1. Characteristics of Iron-Based Nanoparticles

Co-precipitation [23], thermal decomposition [24], hydrothermal reactions [25], microemulsion [26], sol-gel [27] are common methods to produce iron nanoparticles. Of all, thermal decomposition and hydrothermal reactions perform well in uniformity and shape [28]. Iron nanoparticles with controlled size can be synthesized from several to dozens. Iron nanoparticles have stronger magnetization with a larger size in some extent in theory [29]. For example, Y Jun found 4 nm, 6 nm, 9 nm, 12 nm magnetic  $\text{Fe}_3\text{O}_4$  nanosphere’s transverse relaxivities  $R_2$  value, synthesized through thermal decomposition of iron acetylacetonate ( $\text{Fe}(\text{acac})_3$ ), changed from 78 to 106, 130, and 218  $\text{mM}^{-1}\text{s}^{-1}$  [30] (Figure 2). Thermal decomposition of iron carbonyl ( $\text{Fe}(\text{CO})_5$ ) formed 8 nm, 23 nm, 37 nm and 65 nm iron nanoparticles with  $R_2$  174, 204, 240, 249  $\text{mM}^{-1}\text{s}^{-1}$  respectively [31]. Different shapes of INOPs can also be synthesized by changing temperature, pH, solvent, concentration of the precursors to improve relaxation rate and meet different drug delivery needs [32,33]. J Mohapatra found the  $R_2$  values of  $\text{Fe}_3\text{O}_4$  nanorods with lengths of 30, 40, 50, 60 and 70 nm are 312, 381, 427, 545 and 608  $\text{mM}^{-1}\text{s}^{-1}$  respectively [34]. N Lee synthesized 22 nm water-dispersible ferrimagnetic iron oxide nanocubes with  $R_2$  761  $\text{mM}^{-1}\text{s}^{-1}$  showing superior  $T_2$  contrast effect [35]. Moreover, 30 nm octapod iron oxide nanoparticles exhibit  $R_2$  with 680  $\text{mM}^{-1}\text{s}^{-1}$  [36]. Most synthesized iron nanomaterials, prepared in organic solvents, are hydrophobic. However, they need to be water-soluble for medical application. Surface modification is one of the tools to do this. Moreover, surface materials have great influence on hydrodynamic diameter and surface charge, crucial in cell uptake [37]. They also provide functional groups for drugs loading. Surface coatings endow nanoparticles with specific functions, such as lysosomal escape and various stimuli-responsive release, which will be discussed in detail in the part of “Application of Different Coating of INOPs in Cerebral Theranostics”.

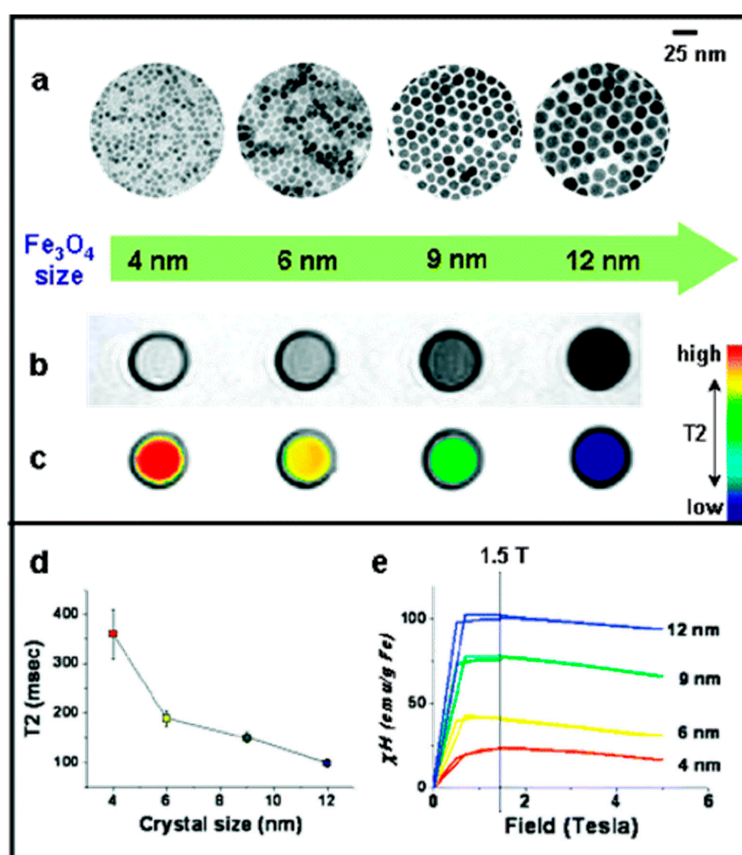


**Figure 2.** Nanoscale size effect of nanocrystals on magnetism and induced Magnetic Resonance (MR) signals. (a) Transmission Electron Microscope (TEM) images of Fe<sub>3</sub>O<sub>4</sub> nanocrystals of 4 to 6, 9, and 12 nm. (b) Size-dependent T<sub>2</sub>-weighted MR images of nanocrystals in aqueous solution at 1.5 T. (c) Size-dependent changes from red to blue in color-coded MR images based on T<sub>2</sub> values. (d) Graph of T<sub>2</sub> value versus nanocrystal size. (e) Magnetization of nanocrystals measured by a superconducting quantum interference device (SQUID) magnetometer. Reproduced from “Nanoscale size effect of magnetic nanocrystals and their utilization for cancer diagnosis via magnetic resonance imaging”, with permission from American Chemical Society, 2005.

### 1.2. Treatment Difficulties and Current Solutions of Brain Diseases

BBB is tightly composed of neuronal pericytes, perivascular astrocytes, and brain capillary endothelial cells (BCECs), limiting drug absorption (Figure 3B) [11]. High levels of active efflux transport proteins, including p-glycoprotein (P-gp), multidrug resistance protein-1 (MRP-1), and breast cancer resistance protein (BCRP) are expressed (Figure 3A). There are several mechanisms for non-invasive drug delivery: (1) passive transportation across the membrane along the concentration gradient through paracellular or transcellular (Figure 3D); (2) receptor mediated endocytosis (Figure 3E), such as transferrin receptor (TfR) [38], lactoferrin receptor (LfR) [39], lipoprotein receptor-related protein (LRP) [40], membrane  $\gamma$ -glutamyl transpeptidase (GGT) [41]; (3) adsorptive mediated endocytosis (Figure 3F), such as trans-activating transcriptional (TAT) peptides [42]; (4) carrier mediated transport (Figure 3C), such as amino acid transporter 1 (EAAT1) [43] and glucose transporters (GLUT1) [44–46]. Small lipophilic molecules, less than 400–500 Da and less than nine hydrogen bonds, can cross BBB by passive transportation. However, most larger nutrients cross BBB with the aid of carrier molecules [20].

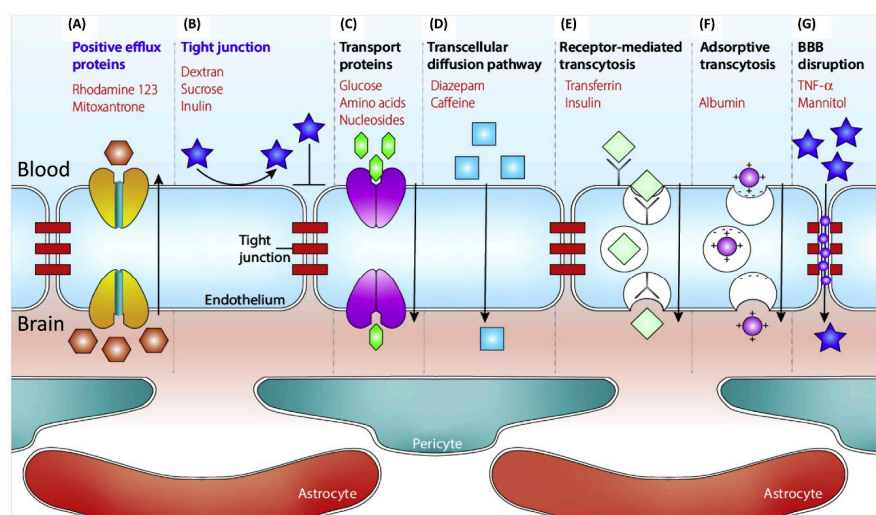


**Figure 3.** BBB transport pathways. A schematic diagram of endothelial cells (ECs), pericytes, and astrocytes forming the BBB. (A) The activity of efflux transport proteins such as p-glycoprotein (P-gp). (B) Selective permeability of tight BBB. (C) Carrier mediated pathway. (D) Passive transportation. (E) Receptor mediated pathway. (F) Adsorptive mediated pathway. (G) Natural occurring biomolecules increase the permeability of the brain endothelium. Reproduced from “Advanced in Microfluidic Blood-Brain Barrier (BBB) Models”, with permission from Elsevier, 2019.

## 2. Application of Different Coating of INOPs in Cerebral Theranostics

Brain diseases are hard to treat because of BBB, and many iron nanoparticles are designed to overcome this difficulty [47–49]. Of all, gliomas [50–53], Alzheimer’s disease (AD), Parkinson’s disease (PD) [54–56] are widely studied. Glioma, especially glioblastoma multiforme, has poor prognosis after common surgical resection, adjuvant chemotherapy, or novel adjuvant therapy combination. Nanomedicine opens a new way for the treatment of glioma in overcoming BBB. Neurodegenerative diseases, as central nervous system (CNS) diseases, exhibit progressive cognitive impairment, loss of memory [57]. The cause of the disease is complex, mainly reported to be abnormal accumulation of protein in the brain [58]. For AD, FDA-approved treatments focus on cholinesterase (donepezil) [59], and N-Methyl-D-Aspartic Acid (NMDA) receptors(memantine) [60]. Many researches on reducing A $\beta$  plaque-secretase modulators (BACE1 [60–63]), hyperphosphorylation tau protein [64,65], inflammation [66,67], other oxidative molecules (metal ion [68], peroxide [69]) have been studied. For PD,  $\alpha$ -syn abnormal aggregation causing impaired motor function with slow movements and tremor [70], studies mainly concentrate on dopamine [71]. Combining those mechanism molecules with ligands overcoming BBB, iron nanoparticles make a great contribution to cerebral disease treatment and diagnosis.

To change the surface charges and hydrophobicity it is possible to increase biocompatibility, endow INOPs with the ability to target and release on demand (Table 1). Different kinds of surface coatings are developed. Here we will discuss the application of different coated INOPs in the treatment of AD, PD, and glioma.

### 2.1. Small Molecules Coating

The presence of numerous OH<sup>-</sup> on the surface of INOPs provides a chance for the attachment of small molecules and surfactants, which can maintain a small hydrodynamic radius, retain the original magnetic properties and improve hydrophilicity at the same time [72]. The ligand- and phase-exchange reactions are the most conventional methods for small molecules modification. Catechol, carboxylic, phosphate, sulfate, and citrate [73] have strong binding force with INOPs so that they can exchange

with the surface organic groups of INOPs like oleic acid or oleylamine. They also perform well as tail of polymers like poly (ethylene glycol) (PEG), polyethyleneimine (PEI).

### 2.1.1. Silicon

Silicon is one of the most widely studied small molecule coatings. Silane can be covalently bound to the surface of INOPs using the reaction of alkoxy silane functions ( $-\text{Si}-\text{O}-\text{R}$ , where R is commonly  $-\text{CH}_3$  or  $-\text{CH}_2-\text{CH}_3$ ) with hydroxyl group of INOPs [74,75]. Further crosslinking events produce a thin inorganic silica layer around the particles. There are four approaches to prepare INOPs@SiO<sub>2</sub>, Stöber method, microemulsion, aerosol pyrolysis, and methods based on sodium silicate solution [28]. Silica coating turns hydrophobic iron nanoparticles into hydrophilic ones [76], reducing aggregation and improving stability. And surface silanol groups facilitate grafting of functional groups [77]. Modified silane, such as 3-aminopropyltriethoxysilane (APTES), p-aminophenyl trimethoxysilane mercaptopropyltriethoxysilane (MPTES), and 2-(carboxymethylthio) ethyltrimethylsilane, is often used for transferring  $-\text{NH}_2$ ,  $-\text{SH}$  and  $-\text{COOH}$  groups to naked iron oxide NPs, respectively [78], which is suitable for further modification with drugs or targets. APTES was beneficial to maintain the morphology of Fe<sub>3</sub>O<sub>4</sub> while MPTES modification resulted in a slight decrease in saturation magnetization [79]. Silane can also perform well as the tail of polymers instead of forming a silicon coating.

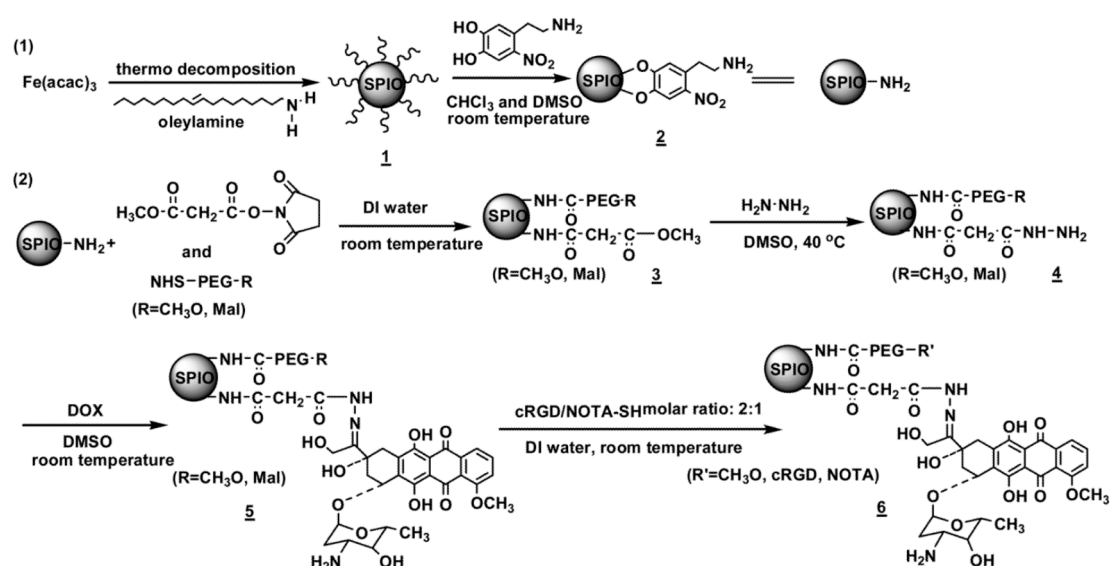
The result of thermotherapy using dextran and amino-silane coated INOPs revealed that amino-silane coated INOPs prolonged the survival time by 4.5-fold over dextran-INOPs in malignant glioma rat [80]. PEG with terminal silane coated INOPs were connected to Alexa Fluor 680 (AF680) fluorochrome using chlorotoxin (CTX) as target molecule, showing no difference in cell toxicity compared with untreated group in C6 glioma cell [81]. PEG-INOPs-AF680/CTX reduced the expression of matrix metalloproteinase 2 (MMP-2) by 40% in glioma cell surface, which is an essential component in the glioma cell invasion pathway. Further crosslinking of silane produced SiO<sub>2</sub> coated INOPs. INOPs@SiO<sub>2</sub> covalently modified with interleukin-6 receptor targeting peptides (I6P7) was used as MRI probe for glioma. Its positive charge was favorable for BBB crossing, increasing the accumulation in the tumor region [82]. Gold and iron oxide NPs in the hollow of silica golf balls (MGNS) was made to deliver Dox before encapsulation in heat and pH sensitive polymer poly (N-isopropylacrylamide co methacrylic acid) (p (NIPAM-co-MAA)), enhancing drug uptake of neurons in the magnetic field [83].

### 2.1.2. Catechol

Inspired by natural phenomena, catechol-derived ligands for INOPs have been developed. Dopamine and its modifications are important catechol. Rajh et al. believed dopamine assembled on Fe<sub>2</sub>O<sub>3</sub> nanoparticles by bidentate chelating interaction [84]. In weak alkaline solution, dopamine is prone to self-oxidation, resulting in attached PDA coating. PDA coating exhibits a special zwitterionicity: it is positively charged at low pH while it turns to be negative at high pH, which has potential application in drug delivery [85]. Moreover, dopamine can also have functions as the tail of other polymers.

Caffeic acid (3,4-dihydroxy-cinnamic acid, CA), with positive biological effects such as anti-oxidant, anti-inflammatory, anti-HIV, anti-tumor, and anti-metastatic effects was used as coating of INOPs due to its strong affinity for INOPs, which could make anti-oxidant drugs keep for at least 45 min in the brain [86]. It plays dual functions as both small surface coating and anti-oxidant drug. Nitrodopamine anchored INOPs were made to deliver anti-cancer drug Dox and a macrocyclic chelating agent (1,4,7-triazacyclononane-N, N', N''-triacetic acid, NOTA) before conjugation with targeting peptide-cyclic arginine-glycine-aspartic acid (cRGD) peptide (Scheme 1). The transverse ( $R_2$ ) relaxivities of nanoparticles ( $101.9 \text{ mM}^{-1}\text{s}^{-1}$ ) was slightly lower than that of FDA approved dextran-coated Feridex ( $111.5 \text{ mM}^{-1}\text{s}^{-1}$ ). Nanoparticles exhibited a higher cellular uptake, leading to higher cytotoxicity [87].





**Scheme 1.** Procedures used to prepare the multifunctional nitrodopamine anchored iron oxide nanoparticles (INOPs) nanocarriers. Reproduced from “cRGD-functionalized, DOX-conjugated, and  $^{64}\text{Cu}$ -labeled superparamagnetic iron oxide nanoparticles for targeted anticancer drug delivery and PET/MR imaging”, with permission from Elsevier, 2011.

## 2.2. Polymers Coating

INOPs coating can be obtained through lots of approaches, such as in situ coating, ligand exchange, post-synthesis adsorption, post-synthesis end grafting [88], and so on. To date, many polymers coatings have been developed via surface coverage or forming micelles. Dextran, chitosan, polyethylene glycol (PEG), polyvinyl alcohol (PVA), polydopamine (PDA), polysaccharide, polyethyleneimine (PEI), polyvinylpyrrolidone (PVP), and polyamidoamine (PAMAM) are common surface coverage polymers used in the coating of INOPs [28]. Dextran, PEG, or their modifications coated INOPs have been clinically approved or approved in clinical test (Figure 4a).

To combine the advantages of different polymers, copolymers are developed. For example, copolymers of PEG and PEI have both the ability to load gene and prolong half-life in blood [89]. Copolymers of PLGA and PEG can help nanoparticles escape from the endo-lysosomal compartment to the cytoplasmic compartment and reduce hydrophobicity of PLGA [90]. Amphiphilic block copolymers have facilitated the preparation of iron-based micellar drug carrier systems by self-assembly of the copolymers in aqueous solution to generate polymeric micelles with diameters of 10–100 nm. The hydrophobic blocks are in the core with hydrophilic block forming shell, reducing interactions with proteins and prolonging blood circulation time. Such micelle provides hydrophobic space for hydrophobic iron nanoparticles (Figure 4). If the concentration of copolymer is above the critical micelle concentration (CMC), micelles are formed in various shapes, and the shapes depend on the temperature, polymer concentration, pH, ionic strength of the solution, and so on [4]. Various amphiphilic block copolymers have been developed to coat iron nanoparticles by copolymerization of common polymers, such as PEG, poly(carboxybetaine) (PCB), poly(lactide-co-glycolide) (PLGA), poly(ethylene oxide) (PEO), poly(3-caprolactone) (PCL), poly(l-lactic acid) (PLLA), N-(2-hydroxypropyl) methacrylamide (HPMA), poly( $\epsilon$ -caprolactone) etc. Moreover, stimuli-sensitive amphiphilic block copolymers have been designed to control release of drugs.

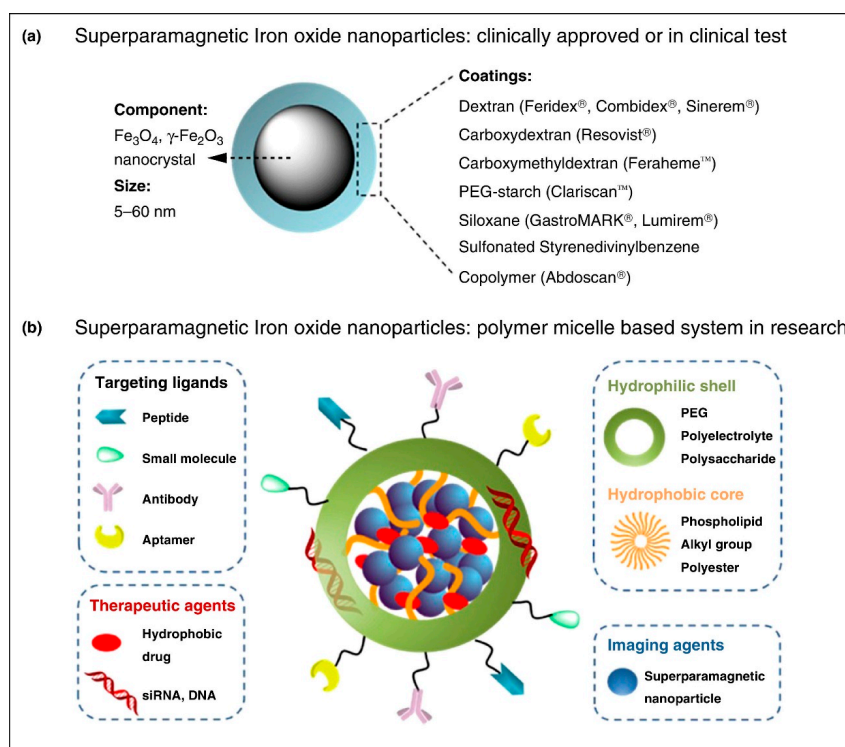


**Figure 4.** Schematic illustration of the polymer micelle composite system of surface-engineered superparamagnetic iron oxide nanoparticles (SPION) for imaging and therapy application. (a) Clinically approved or in clinical test SPION with biocompatible coatings and iron oxide cores; for each kind of coating material, commercial products are listed aside. (b) Amphiphilic polymers to form a micelle structure with hydrophilic shell and hydrophobic core. INOPs and hydrophobic drugs are packed into the core, targeting ligands can be coupled onto the hydrophilic surface. Reproduced from “Superparamagnetic iron oxide nanoparticles for MR imaging and therapy: design considerations and clinical applications”, with permission from Elsevier, 2014.

### 2.2.1. Dextran

Dextran-coated superparamagnetic iron oxide nanoparticles (SPIONs) were described in 1982 by in-situ technology and have been approved by Food and Drug Administration (FDA) [91]. Carboxymethyl-dextran (CMD) coated SPIONs were synthesized to connect with anti-CD44 antibody, whose contents of CMD influence its stability [92]. Dual-crosslinked amine activated dextran (AMD) coated SPIONs increased molecular weight of the coating and improved the dispersion [93]. Dextran coated INOPs were treated with epichlorohydrin to prevent dextran dissociation, which could produce cross-linked iron oxide nanoparticles (CLIO) with a high circulation half-life in blood and no acute toxicity [94].

Dextran and its modifications are used in the study of cerebral disease. Stem cell therapeutics for PD focus on the differentiation of mesenchymal stem cells (MSCs) to dopaminergic (DA) producing cells, replacing damaged DA neurons in PD. Dextran-coated or dextran-derivatives-coated iron oxide (IO) nanoparticles (NPs) (Dex-IO NPs) can activate the tropism of human MSCs (hMSCs) from bone marrow toward tumor [95]. A combination of dextran sulfate coated INOPs and quercetin was less toxic to PC12, a cell line readily quantifiable, rapid, and reversible response to nerve growth factor (NGF) [96], than dimercaptosuccinic acid (DMSA)-coated INOPs. In detail, dextran sulfate coated INOPs with concentration less than 50  $\mu\text{g}/\text{mL}$  had no significant toxicity to PC12 cells while 1.5 mM DMSA modified INOPs were very toxic to PC12 cells [97].

### 2.2.2. Chitosan

Chitosan (CS) is another important polysaccharides coating, providing positive charge for cell adsorption and opening tight junctions between epithelial cells, thus facilitating transportation [98]. Sterically stabilized chitosan-coated iron nanospheres were obtained after synthesis because of the low solubility of chitosan in the pH of INOPs synthesis [99,100]. Chitosan-based INOPs enhanced gene transfection as gene delivery vector [101]. O-carboxymethyl chitosan (CC) bound  $\text{Fe}_3\text{O}_4$  was developed, improving the problem of chitosan's bad solubility [102]. Trimethyl chitosan (TMC) coated SPIONs, TMC and CMD coated INOPs were also produced to delivery siRNA. They found that CMD-TMC-INOPs had little improvement effect on cytotoxicity and siRNA load compared with TMC-INOPs [103]. This may suggest that a monolayer surface coating of polysaccharide is enough for drug circulation. However, dextran-INOPs were further coated by chitosan to increase surface charge [104], indicating the importance of the order in the multilayer coating.

A combinatorial nano-system was made to treat glioblastoma multiforme (GBM). With tumor-specific ligand-transferrin (Tf) as target, CS-INOPs containing antitumor drug doxorubicin (DOX) for cancer cell killing and fluorescent dye Rhodamine B isothiocyanate (RBITC) for simultaneously intracellular fluorescent showed improved cell uptake and cell killing through a concurrence of cell apoptosis and autophagy in the treated tumor U251 cells. The saturation magnetization of INOPs was estimated to be 56.06 emu/g while CS-INOPs and Tf-CS-INOPs were 35.34 and 20.94 emu/g respectively, demonstrating that the saturation magnetization decreased after coating. The apoptosis of U251 MG cells treated with Tf-CS-INOPs were about 70% and the cell viability came down to about 55% [105]. Another bimodal molecular imaging system, overcoming the cons of magnetic (low sensitivity) and fluorescence (low resolution) imaging was made by combining CS-INOPs with CdS. Podophyllotoxin (PD), a naturally occurring antimetabolic agent, was added, too. Deposition of chitosan NPs in lungs no other organs may ascribe to the mucoadhesion property of chitosan [106], which may be resolved by CS modification with other biocompatible molecule.

### 2.2.3. Poly (Ethylene Glycol) PEG

PEG, as a amphiphilic molecule at the size lower than 100 kD [107], is synthesized by anionic ring opening polymerization of ethylene oxide, regarded to be "stealth" molecule to reduce reticuloendothelial (RES) clearance [108], reduce nanoparticle uptake by macrophages [109,110] and extend blood circulation time in vivo, making it suitable for targeted therapy. PEG deposits on the surface of INOPs in situ [111] or grafted PEG connects to INOPs via middle coating, like chitosan, silane [112]. The development of dual function PEG expands its application in coating.

A MGMT inhibitors O6-benzyl guanosine (BGS) covalently attached to PEG-INOPs in a pH-response manner to improve cell sensitivity to TMZ. The combination reduced the cell resistance by approximately 40-fold while BGS reduced resistance by 19-fold, demonstrating BGS-PEG-INOPs' greater sensitivity to TMZ in human GBM cells [113]. Methotrexate (MTX), a short half-life and rapid diffusion drug for various forms of cancer, was covalently bound to  $\text{Fe}_3\text{O}_4$  nanoparticles via a bifunctional PEG with the end of silane and trifluoroethyl ester (TFEE). Intracellular uptake of INOPs-PEG-MTX was higher than NP-dextran in a concentration-dependent manner in glioma [114]. Moreover, PEG-PEI copolymer coated INOPs loaded Dox in a pH-response manner to test the ability of reducing drug efflux in glioma. The  $\text{IC}_{50}$  of INOPs-Dox in C<sub>6</sub>-ADR glioma was approximately 3- to 5-times lower than that of free DOX in cells, demonstrating that preventing drug efflux from drug-resistant cells caused enhanced cell death [115]. PEI-PEG-IONPs loaded salinomycin, an anticancer drug, decreased the glioblastoma cell viability to 45% compared with free-salinomycin's 36% [116].



#### 2.2.4. Polyethyleneimine (PEI)

PEI with highly positive charge is used for gene delivery [117,118]. It has primary, secondary, and tertiary amines, of which two-thirds of the amines can be protonated in a physiological environment, helping escape from endosome due to proton sponge effect and release drugs to cytoplasm [119]. PEI has been widely used in DNA or siRNA gene transfection in vitro [120]. PEI-coated INOPs can be made by in situ, post-synthesis adsorption, or post-synthesis grafting [107]. However, PEI exerts cytotoxic effects on living organisms and short half-life in blood due to non-specific interactions with negatively charged cell-surface, which needs to be considered in its application.

PEI-INOP was made to determine its applicability in gene therapy of brain cancer. The result exhibited no difference in cell toxicity compared with slightly anionic G100 but lower blood concentration [121]. After folic acid-conjugated, cellular uptake was increased [122]. Another research used citraconic anhydride to block primary amine group of PEI, eliciting a pH-sensitive cytotoxic effect in the acidic tumor microenvironment. The study demonstrated lower toxicity of PEI to cell in pH 7.4. Gene silencing effect of siRNA in pH 7.4 and pH 6.2 was 93.8% and 50.8% respectively, making it a pH-response gene silencing nanoparticles (NPs) [123]. INOPs, coated with PEG-grafted chitosan and PEI, functionalized with chlorotoxin (CTX), were used to delivery siRNA. Cells, treated with NP/PEG-CS/PEI-siRNA, exhibited a 53.5% reduction in gene expression compared with a reduction of 88.7% in no siRNA, making NP/PEG-CS/PEI-siRNA a platform for glioma gene therapy [124]. A high drug-loading system was made by combining PEI with phenylboronic acid (PBA) to treat glioma. The Dox loading of PBA-PEI-INOPs was 2.26 and 3.27 times greater than that of PBA-INOPs and PEI-INOPs [125]. Based on PEI, the cationic redox-sensitive PEI (SSPEI) was developed to reduce cytotoxicity. The cell viability of SSPEI-INOPs-pDNA was 8 times than that of PEI and gene transfer efficiency was a little better than PEI in the presence of magnet, showing better biocompatibility in no reduction of transfection efficiency [126].

#### 2.2.5. Poly (Carboxybetaine) PCB

PCB has both cationic and anionic groups, endowing it with the charge-reversible ability in different pH. It is neutral in physiological condition, resisting nonspecific protein adsorption, which changes to positive charge via protonation in acidic environment, helping escape from lysosome [127]. These characteristics make it a special coating for INOPs.

Simvastatin covalently connected ROS-response PCB (Sim-se-se-PCB) was constructed to load hydrophobic SPIONs and absorb negative let-7b antisense oligonucleotide, reducing the differentiation of exogenous neural stem cells (NSCs) and enhancing the secretion of brain-derived neurotrophic factor (BDNF) synergistically. The transfection efficiency of PCB-Se-Se-Sim/let-7b NPs was comparable to that of Lipofectamine 2000 and significantly (170.8%) increased the BDNF level in the culture medium, which further induced the proliferation of NSCs and rescued the memory deficits in 2× Tg-AD mice [128].

Based on PCB, other copolymers were designed to form INOPs-loaded micelles. PCB-poly (2-hydroxyethyl methacrylate)-poly (carboxybetaine) (PHEMA-PCB) polymers were constructed to coat INOPs and delivery retinoic acid (RA) and siRNA (SOX-9), reducing the inhibition the effect of retinoic acid. NPs caused knock-down of approximately 52.3% of SOX-9 mRNA compared with negative controls and significantly improved the learning and memory of AD mice [129] (Figure 5).

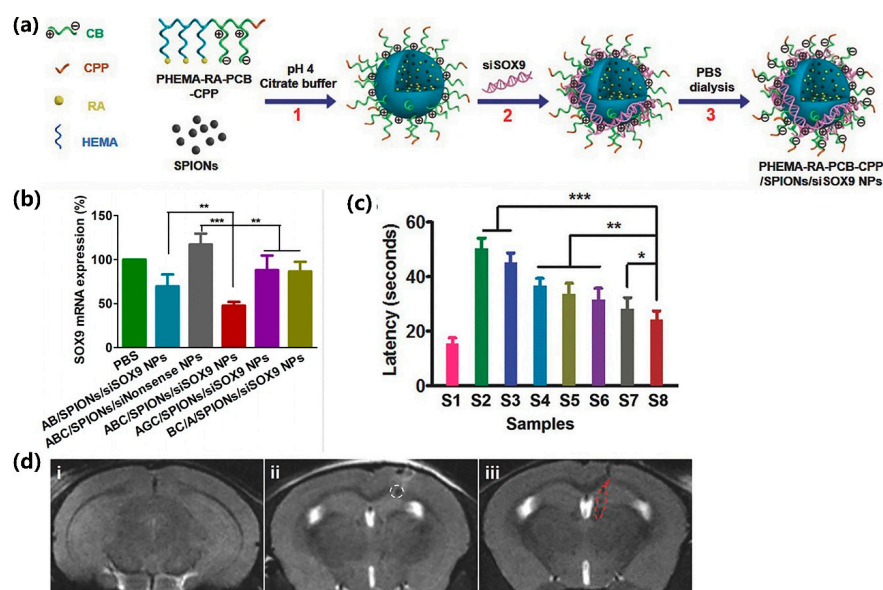


**Figure 5.** (a) Preparation of siRNA-RA NPs. (b) Knockdown the expression level of SOX-9 mRNA. (c) The latency in target quadrant in Morris water maze (MWM). (d) Representative in vivo  $T_2$  MRI images of brains with PHEMA-RA-PCB-CPP/SPIONs/siSOX-9 NPs. (S1) wild, (S2) PBS, (S3) NSCs alone, (S4) PHEMA-RA-PCB-CPP/SPIONs/si-nonsense NPs NSCs, (S5) PHEMA-PCB-CPP/RA/SPIONs/siSOX-9 NPs NSCs, (S6) PHEMA-RA-PEG-CPP/SPIONs/siSOX-9 NPs NSCs, (S7) PHEMA-RA-PCB/SPIONs/siSOX-9 NPs NSCs, and (S8) PHEMA-RA-PCB-CPP/SPIONs/siSOX-9 NPs NSCs. \*  $p < 0.05$ , \*\*  $p < 0.01$ , and \*\*\*  $p < 0.005$  ( $n = 5$ ) versus control. Reproduced from “Traceable Nanoparticle Delivery of Small Interfering RNA and Retinoic Acid with Temporally Release Ability to Control Neural Stem Cell Differentiation for Alzheimer’s Disease Therapy”, with permission from John Wiley and Sons, 2016.

### 2.2.6. PLGA

PLGA is a copolymer of poly lactic acid (PLA) with poly glycolic acid (PGA). It is highly biocompatible and has been approved by FDA as drug delivery vehicles [130]. Various types of block copolymers of PLGA with PEG have been developed, such as PLGA-PEG, PEG-PLGA-PEG [130]. PEG-PLGA coated INOPs were used to delivery PTX as anti-glioma drug. NPs accumulated in liver, but aspartate aminotransferase (AST) level returned to normal after a week, indicating the biocompatibility of PEG/PLGA-INOPs. PTX-PEG/PLGA-INOPs showed less toxicity than PTX [131].

Polymers provide a promising future in the application of INOPs in cerebral disease after targeting and drugs loading. However, the coating materials may cause low magnetic properties. And the blood concentration of NPs is low, which may cause disassembly of micelle before reaching the target.

### 2.3. Lipid Molecule Coating

Lipid, as the constituent of cellular membranes, provides a biocompatible protective barrier for nanoparticles. It can form a closed double layer structure in aqueous solution containing hydrophilic and hydrophobic space. There are two embedding methods for iron nanoparticles, in the phospholipid bilayer or in the core (Figure 6). Research found that these magnetic liposomes had high resistance against intracellular degradation compared with dextran- or citrate-coated particles [132]. Adding PEG-modified phospholipid provides an opportunity for drug, target, or other functional groups binding [133,134] and prolongs blood circulation time, facilitates tumor accumulation via enhancing permeability and retention (EPR) effect [135]. Zwitterionic polymer poly(carboxybetaine) (PCB) modified distearyl phosphatidylethanolamine (DSPE) increased the cell uptake and promoted lysosomal drug release compared with PEG [136].

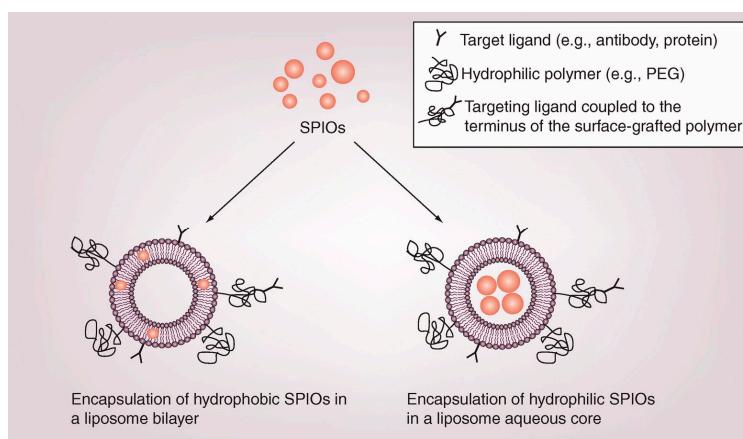


**Figure 6.** Diagram of superparamagnetic iron oxide nanoparticles (SPIONs) encapsulated by liposome. Reproduced from “Liposome-nanoparticles hybrids for multimodal diagnostic and therapeutic applications”, with permission from Future Medicine Ltd., 2007.

Numerous studies have been done on the brain application of DSPE-PEG based iron liposome. DSPE-PEG-B6, high affinity for transferrin receptor (TfR), DSPE-PEG-Mazindol (MA), a high affinity dopamine transporter, DSPE-PEG-phenylboronic acid, loading epigallocatechin gallate (EGCG), and INOPs were self-assembled to treat PD. With the help of MA, NPs were internalized into dopaminergic neurons after crossing BBB with help of B6. In the ROS environment of dopaminergic neurons, EGCG played the role of anti  $\alpha$ -synuclein ( $\alpha$ S) aggregation and promoting neurotransmitter circulation. INOPs functioned as MR imaging. NPs reduced  $\alpha$ S aggregation compared to cells treated with only EGCG and obtained good therapeutic efficacy in PD [137]. Testing reagents and drugs have also been delivered by DSPE-PEG formed INOPs. Congo red, specifically detecting amyloid plaques that have extensive  $\beta$ -sheet structures, and rutin, a glycone of quercetin with the ability of interfering with A $\beta$  aggregation and reducing neurotoxicity, were delivered by DSPE-PEG formed iron-contained liposomes, coinjected with mannitol to treat AD. The cell viability of A $\beta$ <sup>+</sup>Cu<sup>2+</sup> cells improved to 91% from 63% and had a greater contrast-to-noise ratio of MRI. NPs could significantly rescue memory deficits in AD transgenic mice [138]. Different from INOPs in the core, INOPs were produced in the hydrophobic region of phospholipid bilayer with quantum dots (QDs), a new optical imaging method for molecular tracing and biomedical diagnostics, and cilengitide (CGT), inhibiting overexpress of integrin receptors. Using ultrasound-targeted microbubble destruction for delivery, the median survival of glioma rat was significantly extended to 59.6d compared with the control's (20d) [139].

Lipid coating provides more biocompatible modification for INOPs. Besides, it can encapsulate lots of INOPs and deliver them to the target site, avoiding dilution like micelle, resulting in a high concentration of drugs for therapy and INOPs for imaging.

#### 2.4. Lipid and Polymers Coating

INOPs in the core of liposomes need to be hydrophilic. Polymers are one of the methods to change INOPs from hydrophilicity to hydrophobicity, which provide a chance for the combination of lipid and polymers. Moreover, different from supported lipid bilayers (SLB), the inner and the outer leaflet being composed of the same molecules, hybrid lipid bilayer (HLB) is composed of different molecules where the composition of the two leaflets are not identical and only the outer leaflet actually contains lipid molecules, adapting a lipid-bilayer-like arrangement [140]. The combination of lipid and polymers are also applied in HLB. In addition, amphiphilic lipid can also self-assembly into micelles with polymers. DSPE-PEG micelles have greater stability because of interaction of hydrophobic acyl chains in phospholipid fragments, making the CMC of DSPE-PEG micelle 100-fold lower than the CMC of polymeric micelles fabricated from other block copolymers [141,142]. More hydrophobic

drugs are possible to be loaded because of the hydrophobicity conferred by the diacyl lipid chains [143]. The addition of lipid in polymers increased the biocompatibility of NPs.

Three drugs, Dox, combretastatin A4 (CA4), and all-trans retinoic acid (ATRA) were combined through pH-sensitive poly ( $\beta$ -amino ester) (PAE), hypoxic-response azobenzene (AZO) and hydrophobic interaction together with IONPs delivered in the core of DSPE-PEG and PAE constituted micelle to release in order. CA4 was released in GBM acid environment to destroy the angiogenesis after B6 mediated BBB crossing. Then ATRA and Dox played their roles of enhancing GSCs differentiating to glioblastomas and killing them after PAE-mediated lysosomal escape. NPs extended the circulation time of the drugs and maintained survival rate at 60% after treating compared with dying in other groups [144]. After the development of PCB with good lysosomal escape ability, DSPE-PCB based lipid envelope was constructed. Focusing on the immunosuppressive tumor microenvironment at the same time of chemotherapy in glioblastoma, INOPs were encapsulated in the core with siRNA (TGF- $\beta$ ) on the hydrophilic surface of the micelle formed by an ROS-responsive polymer poly[(2-acryloyl) ethyl (p-boronic acid benzyl) diethylammonium bromide] (BA-PDEAEA, BAP) before coated with TMZ loaded DSPE-PCB liposome. After the ANG-2 mediated BBB crossing and PCB-mediated lysosomal escaping, TMZ and TGF- $\beta$  were released to kill tumors. The NPs reduced TGF- $\beta$  by 44% and maintained 80% survival while the others died [145] (Figure 7).

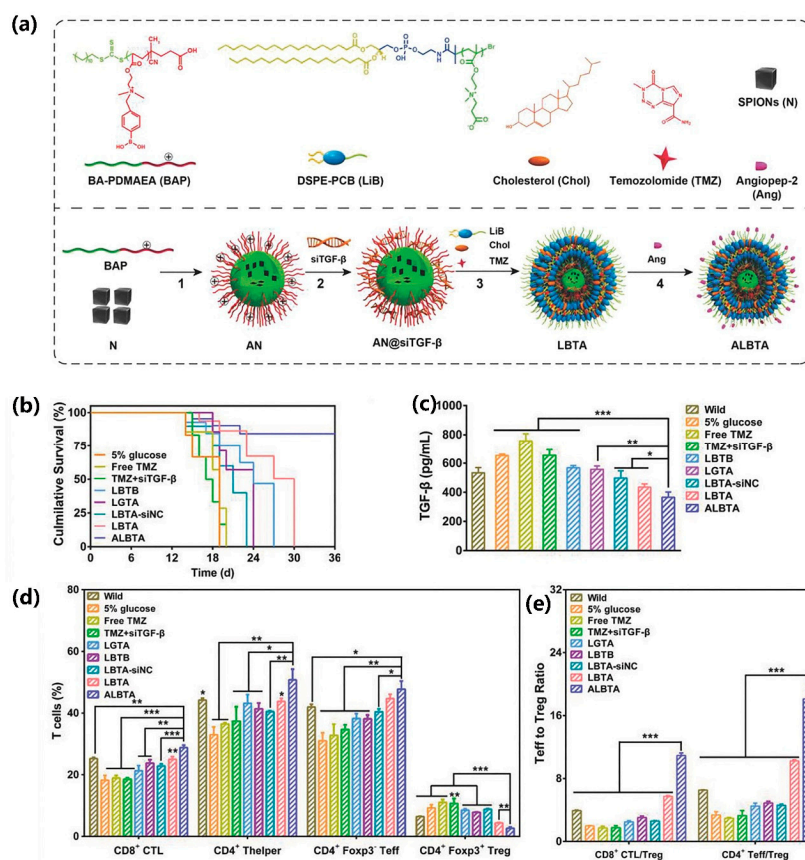


**Figure 7.** (a) Preparation of DSPE-PCB coated BAP/SPIONs@siTGF- $\beta$  NPs. (b) T cell composition of different groups. (c) CD8<sup>+</sup> cytotoxic lymphocyte cells (CTL): Treg ratios and CD4<sup>+</sup> effector T cells: Treg ratios in spleen upon various treatments. (d) The survival time of different groups of intracranial glioblastoma-bearing mice after various treatments. (e) The regulation of TGF- $\beta$  secretion after treatment with various formulations in vivo. \*: differences between ALBTA with other groups, \*:  $p < 0.05$ , \*\*:  $p < 0.01$ , \*\*\*:  $p < 0.001$ . Reproduced from “Traceable Nanoparticles with Dual Targeting and ROS Response for RNAi-Based Immunotherapy of Intracranial Glioblastoma Treatment”, with permission from John Wiley and Sons, 2018.



## 2.5. Other Coatings

Other materials are also used to improve iron nanoparticles performance [146]. Au coating was reported to enhance imaging signals and endow the ability of target and function modification [147]. Metal oxides can protect the magnetic nuclei from oxidation, for example, the MgO shell can protect magnetic nuclei from oxidation up to 600 °C [140].

**Table 1.** Summary of different coatings.

Coating Classification	Coating (Examples)	Characteristics
Small molecule	Catechol, carboxylic, phosphate, sulfate, citrate, silane	reducing loss of original magnetic properties [72], antioxidant activity [86]
Polymer	Dextran, Chitosan, PEG, PEI, PCB, PLGA	magnetic reduction [105], providing positive charge [117], reduce reticuloendothelial (RES) clearance [108], proton sponge effect [127]
Lipid molecule	DSPE-PEG, DSPE-PCB	biocompatible protective barrier [132]
Polymer and lipid molecule	BAP + DSPE-PCB PAE + DSPE-PEG	combination of lipid and polymers [141–143]
Other coatings	Au, MgO	function modification [140,147]

The negatively charged polydopamine (PDA) coated  $\text{Fe}_3\text{O}_4$  was coated with positively charged p53 plasmid-loaded poly (2-dimethyl amino) ethyl methacrylate (PDM)-coated Au through consecutive electrostatic assembly. The C6 glioma cell viability decreased to 24.1% by combining PTT with gene therapy in vitro and produced an effective inhibition of high-proliferation-rate C6 glioma in vivo [148] (Figure 8).

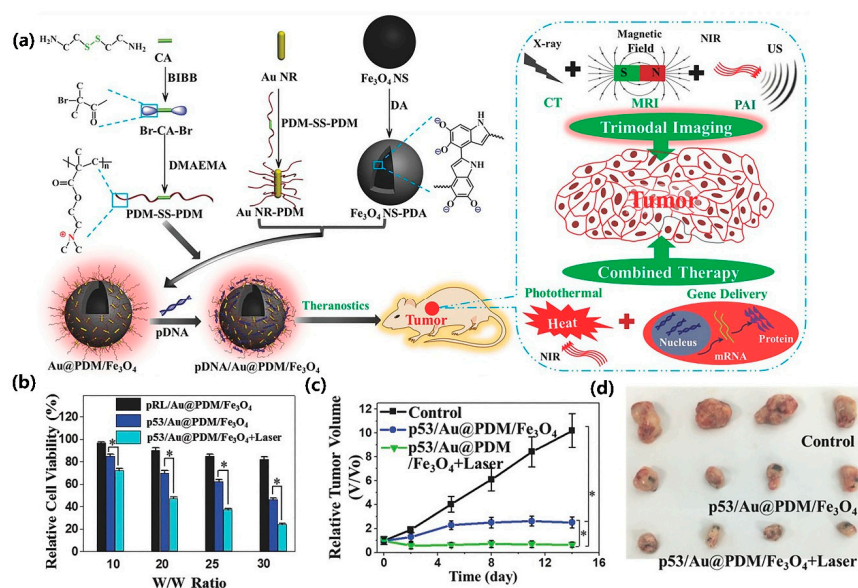


**Figure 8.** (a) Preparation of Au coated  $\text{Fe}_3\text{O}_4$ . (b) Cell viability of C6 cells after various treatments. (c) The C6 tumor growth curves of mice after various treatments, where the tumor volumes were normalized to their initial tumor sizes (mean  $\pm$  SD,  $n = 4$ ). (d) Photographs of (c).  $p$  values were calculated by the student's test: \*  $p < 0.05$ . Reproduced from "Multifunctional pDNA-Conjugated Polycationic Au Nanorod-Coated  $\text{Fe}_3\text{O}_4$  Hierarchical Nanocomposites for Trimodal Imaging and Combined Photothermal/Gene Therapy", with permission from John Wiley and Sons, 2016.

## 3. Conclusions and Prospecction

Iron-based nanoparticles are promising targeted drug carriers for theranostics of brain diseases. After surface modification, they have the abilities to (1) encapsulate multiple therapy molecules,



like gene, protein, chemical drugs to achieve multi-drug cooperation therapy; (2) deliver drugs to target sites to increase drug concentration in disease site; (3) release loaded drugs according to various stimuli conditions of disease site. There have been FDA-approved INOPs [149,150]. For example, Feraheme® has been approved for iron deficiency anemia in adults [4], which show advantages over other nanoparticles as a component of human body. Ferucarbotran, Ferumoxide, and Ferumoxytol have been approved for central nervous system (CNS) imaging [15], showing the application potential of delivery in central nervous system diseases.

INOPs approved by FDA are in the first generation-imaging. Later, NanoTherm was approved to treat recurrent glioblastoma multiforme in 2010 [15]. There are no FDA-approved INOPs for drug delivery yet. The first consideration is the targeting. Target ligands may not always work because of their deposition in liver and kidney organs when administered intravenously. To solve the problem, further development of administration mode and surface coating will be needed, which can reduce the macrophage-induced phagocytosis and protein interaction. It is exciting that studies have found that therapeutic agents can be delivered to the brain by convention enhanced delivery (CED) at high concentration without much toxicity to normal organs [151]. The second consideration is the drug leakage. Common polymers micelle may be in a state of disassembly when the blood concentration of polymer is below CMC after drug injection, causing quick drug release. In this regard, crosslinked coatings offer a solution [152,153]. Moreover, the development of iron-based nanoparticles largely depends on uniformity and size of SPIONs.

**Author Contributions:** Writing—original draft, Y.W.; Writing—review & editing, Y.L., Z.L., J.Y., and X.Z. All authors have read and agreed to the published version of the manuscript.

**Funding:** This work was financially supported by the National High-tech Research and Development Program (2016YFA0200303), the National Natural Science Foundation of China (31771095, 21875254 and 21905283) and the Natural Science Foundation of Beijing Municipality (L172046, 2192057).

**Acknowledgments:** The authors would like to acknowledge the supports from the whole members of Zhang lab and State Key Laboratory of Biochemical Engineering.

**Conflicts of Interest:** The authors declare no conflict of interest.

## References

1. Lu, A.H.; Salabas, E.L.; Schuth, F. Magnetic nanoparticles: Synthesis, protection, functionalization, and application. *Angew. Chem. Int. Ed. Engl.* **2007**, *46*, 1222–1244. [[CrossRef](#)] [[PubMed](#)]
2. Gao, J.; Gu, H.; Xu, B. Multifunctional magnetic nanoparticles: Design, synthesis, and biomedical applications. *Acc. Chem. Res.* **2009**, *42*, 1097–1107. [[CrossRef](#)] [[PubMed](#)]
3. Hao, R.; Xing, R.; Xu, Z.; Hou, Y.; Gao, S.; Sun, S. Synthesis, functionalization, and biomedical applications of multifunctional magnetic nanoparticles. *Adv. Mater.* **2010**, *22*, 2729–2742. [[CrossRef](#)] [[PubMed](#)]
4. Ulbrich, K.; Hola, K.; Subr, V.; Bakandritsos, A.; Tucek, J.; Zboril, R. Targeted drug delivery with polymers and magnetic nanoparticles: Covalent and noncovalent approaches, release control, and clinical studies. *Chem. Rev.* **2016**, *116*, 5338–5431. [[CrossRef](#)]
5. Ho, D.; Sun, X.; Sun, S. Monodisperse magnetic nanoparticles for theranostic applications. *Acc. Chem. Res.* **2011**, *44*, 875–882. [[CrossRef](#)]
6. Amiri, H.; Saeidi, K.; Borhani, P.; Manafirad, A.; Ghavami, M.; Zerbi, V. Alzheimer's disease: Pathophysiology and applications of magnetic nanoparticles as MRI theranostic agents. *ACS Chem. Neurosci.* **2013**, *4*, 1417–1429. [[CrossRef](#)]
7. Lee, H.; Shin, T.H.; Cheon, J.; Weissleder, R. Recent developments in magnetic diagnostic systems. *Chem. Rev.* **2015**, *115*, 10690–10724. [[CrossRef](#)] [[PubMed](#)]
8. Liu, L.; Li, Y.; Liu, R.; Shen, Q.; Li, Y.; Shi, Z.; Shen, J.; Ji, W.; Zhang, X. Switchable nanoparticle for programmed gene-chem delivery with enhanced neuronal recovery and CT imaging for neurodegenerative disease treatment. *Mater. Horiz.* **2019**, *6*, 1923–1929. [[CrossRef](#)]
9. Yousaf, M.Z.; Yu, J.; Hou, Y.L.; Gao, S. Magnetic nanoparticle-based cancer nanodiagnostics. *Chin. Phys. B* **2013**, *22*, 58702. [[CrossRef](#)]

10. Barrow, M.; Taylor, A.; Murray, P.; Rosseinsky, M.J.; Adams, D.J. Design considerations for the synthesis of polymer coated iron oxide nanoparticles for stem cell labelling and tracking using MRI. *Chem. Soc. Rev.* **2015**, *44*, 6733–6748. [[CrossRef](#)] [[PubMed](#)]
11. Luo, S.; Ma, C.; Zhu, M.-Q.; Ju, W.-N.; Yang, Y.; Wang, X. Application of Iron Oxide Nanoparticles in the diagnosis and treatment of neurodegenerative diseases with emphasis on alzheimer's disease. *Front. Cell. Neurosci.* **2020**, *14*, 21. [[CrossRef](#)]
12. Farka, Z.; Jurik, T.; Kovar, D.; Trnkova, L.; Skladal, P. Nanoparticle-based immunochemical biosensors and assays: Recent advances and challenges. *Chem. Rev.* **2017**, *117*, 9973–10042. [[CrossRef](#)] [[PubMed](#)]
13. Deng, H.; Dai, F.; Ma, G.; Zhang, X. Theranostic gold nanomicelles made from biocompatible comb-like polymers for thermochemotherapy and multifunctional imaging with rapid clearance. *Adv. Mater.* **2015**, *27*, 3645–3653. [[CrossRef](#)]
14. Kievit, F.M.; Zhang, M. Surface engineering of iron oxide nanoparticles for targeted cancer therapy. *Acc. Chem. Res.* **2011**, *44*, 853–862. [[CrossRef](#)] [[PubMed](#)]
15. Dadfar, S.M.; Roemhild, K.; Drude, N.I.; von Stillfried, S.; Knuchel, R.; Kiessling, F.; Lammers, T. Iron oxide nanoparticles: Diagnostic, therapeutic and theranostic applications. *Adv. Drug Deliv. Rev.* **2019**, *138*, 302–325. [[CrossRef](#)] [[PubMed](#)]
16. Li, K.; Nejadnik, H.; Daldrup-Link, H.E. Next-generation superparamagnetic iron oxide nanoparticles for cancer theranostics. *Drug Discov. Today* **2017**, *22*, 1421–1429. [[CrossRef](#)]
17. Subramani, K.; Hosseinkhani, H.; Khraisat, A.; Hosseinkhani, M.; Pathak, Y. Targeting nanoparticles as drug delivery systems for cancer treatment. *Curr. Nanosci.* **2009**, *5*, 135–140. [[CrossRef](#)]
18. Meng, X.X.; Wan, J.Q.; Jing, M.; Zhao, S.G.; Cai, W.; Liu, E.Z. Specific targeting of gliomas with multifunctional superparamagnetic iron oxide nanoparticle optical and magnetic resonance imaging contrast agents. *Acta Pharmacol. Sin.* **2007**, *28*, 2019–2026. [[CrossRef](#)]
19. Mizrahy, S.; Gutkin, A.; Decuzzi, P.; Peer, D. Targeting central nervous system pathologies with nanomedicines. *J. Drug Target.* **2019**, *27*, 542–554. [[CrossRef](#)] [[PubMed](#)]
20. Furtado, D.; Bjornmalm, M.; Ayton, S.; Bush, A.I.; Kempe, K.; Caruso, F. Overcoming the blood-brain barrier: The role of nanomaterials in treating neurological diseases. *Adv. Mater.* **2018**, *30*. [[CrossRef](#)] [[PubMed](#)]
21. Li, Y.; Liu, R.; Ji, W.; Li, Y.; Liu, L.; Zhang, X. Delivery systems for theranostics in neurodegenerative diseases. *Nano Res.* **2018**, *11*, 5535–5555. [[CrossRef](#)]
22. Meng, J.; Agrahari, V.; Youm, I. Advances in targeted drug delivery approaches for the central nervous system tumors: The inspiration of nanobiotechnology. *J. Neuroimmune Pharmacol.* **2017**, *12*, 84–98. [[CrossRef](#)]
23. Massart, R. Preparation of aqueous magnetic liquids in alkaline and acidic media. *IEEE Trans. Magn.* **1981**, *17*, 1247–1248. [[CrossRef](#)]
24. Liu, J.; Sun, Z.; Deng, Y.; Zou, Y.; Li, C.; Guo, X.; Xiong, L.; Gao, Y.; Li, F.; Zhao, D. Highly water-dispersible biocompatible magnetite particles with low cytotoxicity stabilized by citrate groups. *Angew. Chem. Int. Ed.* **2009**, *48*, 5875–5879. [[CrossRef](#)]
25. Rockenberger, J.; Scher, E.C.; Alivisatos, A.P. A new nonhydrolytic single-precursor approach to surfactant-capped nanocrystals of transition metal oxides. *J. Am. Chem. Soc.* **1999**, *121*, 11595–11596. [[CrossRef](#)]
26. Mohagheghpour, E.; Moztarzadeh, F.; Rabiee, M.; Tahiri, M.; Ashuri, M.; Sameie, H.; Salimi, R.; Moghadas, S. Micro-Emulsion synthesis, surface modification, and photophysical properties of Zn<sub>1-x</sub>Mn<sub>x</sub>S nanocrystals for biomolecular recognition. *IEEE Trans. Nanobioscience* **2012**, *11*, 317–323. [[CrossRef](#)] [[PubMed](#)]
27. Lemine, O.M.; Omri, K.; Zhang, B.; El Mir, L.; Sajieddine, M.; Alyamani, A.; Bououdina, M. Sol-gel synthesis of 8 nm magnetite (Fe<sub>3</sub>O<sub>4</sub>) nanoparticles and their magnetic properties. *Superlattices Microstruct.* **2012**, *52*, 793–799. [[CrossRef](#)]
28. Zhu, N.; Ji, H.; Yu, P.; Niu, J.; Farooq, M.U.; Akram, M.W.; Udego, I.O.; Li, H.; Niu, X. Surface modification of magnetic iron oxide nanoparticles. *Nanomaterials* **2018**, *8*, 810. [[CrossRef](#)] [[PubMed](#)]
29. Ni, D.; Bu, W.; Ehlerding, E.B.; Cai, W.; Shi, J. Engineering of inorganic nanoparticles as magnetic resonance imaging contrast agents. *Chem. Soc. Rev.* **2017**, *46*, 7438–7468. [[CrossRef](#)] [[PubMed](#)]
30. Jun, Y.W.; Huh, Y.M.; Choi, J.S.; Lee, J.H.; Song, H.T.; Kim, S.; Yoon, S.; Kim, K.S.; Shin, J.S.; Suh, J.S.; et al. Nanoscale size effect of magnetic nanocrystals and their utilization for cancer diagnosis via magnetic resonance imaging. *J. Am. Chem. Soc.* **2005**, *127*, 5732–5733. [[CrossRef](#)]

31. Mou, Y.B.; Xing, Y.; Ren, H.Y.; Cui, Z.H.; Zhang, Y.; Yu, G.J.; Urba, W.J.; Hu, Q.G.; Hu, H.M. The effect of superparamagnetic Iron Oxide nanoparticle surface charge on antigen cross-presentation. *Nanoscale Res. Lett.* **2017**, *12*, 52. [[CrossRef](#)] [[PubMed](#)]
32. Roca, A.G.; Gutierrez, L.; Gavilan, H.; Fortes Brollo, M.E.; Veintemillas-Verdaguer, S.; del Puerto Morales, M. Design strategies for shape-controlled magnetic iron oxide nanoparticles. *Adv. Drug Deliv. Rev.* **2019**, *138*, 68–104. [[CrossRef](#)] [[PubMed](#)]
33. Andrade, R.G.D.; Veloso, S.R.S.; Castanheira, E.M.S. Shape Anisotropic Iron Oxide-based magnetic nanoparticles: Synthesis and biomedical applications. *Int. J. Mol. Sci.* **2020**, *21*, 2455. [[CrossRef](#)] [[PubMed](#)]
34. Mohapatra, J.; Mitra, A.; Tyagi, H.; Bahadur, D.; Aslam, M. Iron oxide nanorods as high-performance magnetic resonance imaging contrast agents. *Nanoscale* **2015**, *7*, 9174–9184. [[CrossRef](#)] [[PubMed](#)]
35. Lee, N.; Choi, Y.; Lee, Y.; Park, M.; Moon, W.K.; Choi, S.H.; Hyeon, T. Water-dispersible ferrimagnetic Iron Oxide nanocubes with extremely high  $r(2)$  relaxivity for highly sensitive in vivo MRI of tumors. *Nano Lett.* **2012**, *12*, 3127–3131. [[CrossRef](#)]
36. Zhao, Z.; Zhou, Z.; Bao, J.; Wang, Z.; Hu, J.; Chi, X.; Ni, K.; Wang, R.; Chen, X.; Chen, Z.; et al. Octapod iron oxide nanoparticles as high-performance T-2 contrast agents for magnetic resonance imaging. *Nat. Commun.* **2013**, *4*. [[CrossRef](#)]
37. Saito, S.; Tsugeno, M.; Koto, D.; Mori, Y.; Yoshioka, Y.; Nohara, S.; Murase, K. Impact of surface coating and particle size on the uptake of small and ultrasmall superparamagnetic iron oxide nanoparticles by macrophages. *Int. J. Nanomed.* **2012**, *7*, 5415–5421.
38. Marino, A.; Camponovo, A.; Degl'Innocenti, A.; Bartolucci, M.; Tapeinos, C.; Martinelli, C.; De Pasquale, D.; Santoro, F.; Mollo, V.; Arai, S.; et al. Multifunctional temozolomide-loaded lipid superparamagnetic nanovectors: Dual targeting and disintegration of glioblastoma spheroids by synergic chemotherapy and hyperthermia treatment. *Nanoscale* **2019**, *11*, 21227–21248. [[CrossRef](#)]
39. Fang, J.-H.; Chiu, T.-L.; Huang, W.-C.; Lai, Y.-H.; Hu, S.-H.; Chen, Y.-Y.; Chen, S.-Y. Dual-targeting lactoferrin-conjugated polymerized magnetic polydiacetylene-assembled nanocarriers with self-responsive fluorescence/magnetic resonance imaging for in vivo brain tumor therapy. *Adv. Healthc. Mater.* **2016**, *5*, 688–695. [[CrossRef](#)]
40. Du, C.; Liu, X.; Hu, H.; Li, H.; Yu, L.; Geng, D.; Chen, Y.; Zhang, J. Dual-targeting and excretable ultrasmall SPIONs for T-1-weighted positive MR imaging of intracranial glioblastoma cells by targeting the lipoprotein receptor-related protein. *J. Mater. Chem. B* **2020**, *8*, 2296–2306. [[CrossRef](#)]
41. Zhou, Q.; Shao, S.; Wang, J.; Xu, C.; Xiang, J.; Piao, Y.; Zhou, Z.; Yu, Q.; Tang, J.; Liu, X.; et al. Enzyme-activatable polymer-drug conjugate augments tumour penetration and treatment efficacy. *Nat. Nanotechnol.* **2019**, *14*, 799–809. [[CrossRef](#)]
42. Zhao, X.; Shang, T.; Zhang, X.; Ye, T.; Wang, D.; Rei, L. Passage of magnetic tat-conjugated  $\text{Fe}_3\text{O}_4@ \text{SiO}_2$  nanoparticles across in vitro blood-brain barrier. *Nanoscale Res. Lett.* **2016**, *11*. [[CrossRef](#)]
43. Canul-Tec, J.C.; Assal, R.; Cirri, E.; Legrand, P.; Brier, S.; Chamot-Rooke, J.; Reyes, N. Structure and allosteric inhibition of excitatory amino acid transporter 1. *Nature* **2017**, *544*, 446–451. [[CrossRef](#)]
44. Patching, S.G. Glucose transporters at the blood-brain barrier: Function, regulation and gateways for drug delivery. *Mol. Neurobiol.* **2017**, *54*, 1046–1077. [[CrossRef](#)] [[PubMed](#)]
45. Deng, D.; Xu, C.; Sun, P.; Wu, J.; Yan, C.; Hu, M.; Yan, N. Crystal structure of the human glucose transporter GLUT1. *Nature* **2014**, *510*, 121–125. [[CrossRef](#)] [[PubMed](#)]
46. Khan, A.R.; Yang, X.; Fu, M.; Zhai, G. Recent progress of drug nanoformulations targeting to brain. *J. Control. Release* **2018**, *291*, 37–64. [[CrossRef](#)] [[PubMed](#)]
47. Thomsen, L.B.; Thomsen, M.S.; Moos, T. Targeted drug delivery to the brain using magnetic nanoparticles. *Ther. Deliv.* **2015**, *6*, 1145–1155. [[CrossRef](#)] [[PubMed](#)]
48. Mazur, J.; Roy, K.; Kanwar, J.R. Recent advances in nanomedicine and survivin targeting in brain cancers. *Nanomedicine* **2018**, *13*, 105–137. [[CrossRef](#)] [[PubMed](#)]
49. Liu, J.; Huang, C.; He, Q. Pharmaceutical application of magnetic Iron Oxide nanoparticles. *Sci. Adv. Mater.* **2015**, *7*, 672–685. [[CrossRef](#)]
50. Glaser, T.; Han, I.; Wu, L.; Zeng, X. Targeted Nanotechnology in Glioblastoma Multiforme. *Front. Pharmacol.* **2017**, *8*. [[CrossRef](#)] [[PubMed](#)]
51. Pinto, M.P.; Arce, M.; Yameen, B.; Vilos, C. Targeted brain delivery nanoparticles for malignant gliomas. *Nanomedicine* **2017**, *12*, 59–72. [[CrossRef](#)]

52. Bredlau, A.L.; Dixit, S.; Chen, C.; Broome, A.-M. Nanotechnology applications for diffuse intrinsic pontine glioma. *Curr. Neuropharmacol.* **2017**, *15*, 104–115. [[CrossRef](#)] [[PubMed](#)]
53. Zhang, F.; Xu, C.-L.; Liu, C.-M. Drug delivery strategies to enhance the permeability of the blood-brain barrier for treatment of glioma. *Drug Des. Dev. Ther.* **2015**, *9*, 2089–2100. [[CrossRef](#)] [[PubMed](#)]
54. Baranowska-Wojcik, E.; Szwajgier, D. Alzheimer's disease: Review of current nanotechnological therapeutic strategies. *Expert Rev. Neurother.* **2020**, *20*, 271–279. [[CrossRef](#)] [[PubMed](#)]
55. Li, Y.; Chen, Z.; Lu, Z.; Yang, Q.; Liu, L.; Jiang, Z.; Zhang, L.; Zhang, X.; Qing, H. "Cell-addictive" dual-target traceable nanodrug for Parkinson's disease treatment via flotillins pathway. *Theranostics* **2018**, *8*, 5469–5481. [[CrossRef](#)] [[PubMed](#)]
56. Kang, Y.J.; Cutler, E.G.; Cho, H. Therapeutic nanoplatforms and delivery strategies for neurological disorders. *Nano Converg.* **2018**, *5*. [[CrossRef](#)] [[PubMed](#)]
57. Dugger, B.N.; Dickson, D.W. Pathology of Neurodegenerative Diseases. *Cold Spring Harb. Perspect. Biol.* **2017**, *9*, 22. [[CrossRef](#)] [[PubMed](#)]
58. Haeberlein, S.L.B.; Harris, T.J.R. Promising Targets for the treatment of neurodegenerative diseases. *Clin. Pharmacol. Ther.* **2015**, *98*, 492–501. [[CrossRef](#)]
59. Lo, D.; Grossberg, G.T. Use of memantine for the treatment of dementia. *Expert Rev. Neurother.* **2011**, *11*, 1359–1370. [[CrossRef](#)]
60. Shega, J.W.; Ellner, L.; Lau, D.T.; Maxwell, T.L. Cholinesterase inhibitor and N-Methyl-D-Aspartic Acid receptor antagonist use in older adults with end-stage dementia: A survey of hospice medical directors. *J. Palliat. Med.* **2009**, *12*, 779–783. [[CrossRef](#)]
61. Vassar, R. BACE1 inhibitor drugs in clinical trials for Alzheimer's disease. *Alzheimers Res. Ther.* **2014**, *6*. [[CrossRef](#)] [[PubMed](#)]
62. Yan, R.; Vassar, R. Targeting the beta secretase BACE1 for Alzheimer's disease therapy. *Lancet Neurol.* **2014**, *13*, 319–329. [[CrossRef](#)]
63. Ly, P.T.T.; Wu, Y.; Zou, H.; Wang, R.; Zhou, W.; Kinoshita, A.; Zhang, M.; Yang, Y.; Cai, F.; Woodgett, J.; et al. Inhibition of GSK3 beta-mediated BACE1 expression reduces Alzheimer-associated phenotypes. *J. Clin. Investig.* **2013**, *123*, 224–235. [[CrossRef](#)] [[PubMed](#)]
64. Xiong, R.; Wang, X.-L.; Wu, J.-M.; Tang, Y.; Qiu, W.-Q.; Shen, X.; Teng, J.-F.; Pan, R.; Zhao, Y.; Yu, L.; et al. Polyphenols isolated from lychee seed inhibit Alzheimer's disease-associated Tau through improving insulin resistance via the IRS-1/PI3K/Akt/GSK-3 beta pathway. *J. Ethnopharmacol.* **2020**, *251*. [[CrossRef](#)]
65. Zhou, H.; Gong, Y.; Liu, Y.; Huang, A.; Zhu, X.; Liu, J.; Yuan, G.; Zhang, L.; Wei, J.-A.; Liu, J. Intelligently thermoresponsive flower-like hollow nano-ruthenium system for sustained release of nerve growth factor to inhibit hyperphosphorylation of tau and neuronal damage for the treatment of Alzheimer's disease. *Biomaterials* **2020**, *237*. [[CrossRef](#)]
66. Stephenson, J.; Nutma, E.; van der Valk, P.; Amor, S. Inflammation in CNS neurodegenerative diseases. *Immunology* **2018**, *154*, 204–219. [[CrossRef](#)] [[PubMed](#)]
67. Shal, B.; Ding, W.; Ali, H.; Kim, Y.S.; Khan, S. Anti-neuroinflammatory Potential of Natural Products in Attenuation of Alzheimer's Disease. *Front. Pharmacol.* **2018**, *9*, 17. [[CrossRef](#)]
68. Valko, M.; Jomova, K.; Rhodes, C.J.; Kuca, K.; Musilek, K. Redox- and non-redox-metal-induced formation of free radicals and their role in human disease. *Arch. Toxicol.* **2016**, *90*, 1–37. [[CrossRef](#)]
69. Uttara, B.; Singh, A.V.; Zamboni, P.; Mahajan, R.T. Oxidative stress and neurodegenerative diseases: A review of upstream and downstream antioxidant therapeutic options. *Curr. Neuropharmacol.* **2009**, *7*, 65–74. [[CrossRef](#)]
70. Sveinbjornsdottir, S. The clinical symptoms of Parkinson's disease. *J. Neurochem.* **2016**, *139*, 318–324. [[CrossRef](#)]
71. Reich, S.G.; Savitt, J.M. Parkinson's Disease. *Med. Clin. N. Am.* **2019**, *103*, 337–350. [[CrossRef](#)] [[PubMed](#)]
72. Wu, W.; Jiang, C.Z.; Roy, V.A.L. Designed synthesis and surface engineering strategies of magnetic iron oxide nanoparticles for biomedical applications. *Nanoscale* **2016**, *8*, 19421–19474. [[CrossRef](#)] [[PubMed](#)]
73. Zeng, M.; Hu, B.; Chen, J.; Zhang, Z.; Zhang, X.; Fan, Z. Superparamagnetic Iron Oxide Nanoparticles as magnetic resonance imaging contrast agent for myocardial infarction. *J. Biomater. Tissue Eng.* **2016**, *6*, 713–718. [[CrossRef](#)]



74. Lee, H.; Yu, M.K.; Park, S.; Moon, S.; Min, J.J.; Jeong, Y.Y.; Kang, H.-W.; Jon, S. Thermally cross-linked superparamagnetic iron oxide nanoparticles: Synthesis and application as a dual imaging probe for cancer in vivo. *J. Am. Chem. Soc.* **2007**, *129*, 12739–12745. [[CrossRef](#)] [[PubMed](#)]
75. Gao, F.; Zhang, L.L.; Huang, F.R.; Du, L. Investigation on poly (methylsilylene ethynylene phenylene ethynylene) co (tetramethyldisiloxane ethynylene phenylene ethynylene). *Chin. Chem. Lett.* **2010**, *21*, 738–742. [[CrossRef](#)]
76. Sotiriou, G.A.; Hirt, A.M.; Lozach, P.-Y.; Teleki, A.; Krumeich, F.; Pratsinis, S.E. Hybrid, silica-coated, janus-like plasmonic-magnetic nanoparticles. *Chem. Mater.* **2011**, *23*, 1985–1992. [[CrossRef](#)]
77. Liu, H.L.; Li, Y.Y.; Sun, K.; Fan, J.B.; Zhang, P.C.; Meng, J.X.; Wang, S.T.; Jiang, L. Dual-responsive surfaces modified with phenylboronic acid-containing polymer brush to reversibly capture and release cancer cells. *J. Am. Chem. Soc.* **2013**, *135*, 7603–7609. [[CrossRef](#)]
78. He, Q.G.; Zeng, L.; Wu, W.; Hu, R.; Huang, J.K. Preparation and magnetic comparison of silane-functionalized magnetite nanoparticles. *Sens. Mater.* **2010**, *22*, 285–295.
79. Wu, W.; Wu, Z.H.; Yu, T.; Jiang, C.Z.; Kim, W.S. Recent progress on magnetic iron oxide nanoparticles: Synthesis, surface functional strategies and biomedical applications. *Sci. Technol. Adv. Mater.* **2015**, *16*, 43. [[CrossRef](#)]
80. Jordan, A.; Scholz, R.; Maier-Hauff, K.; van Landeghem, F.K.H.; Waldoefner, N.; Teichgraber, U.; Pinkernelle, J.; Bruhn, H.; Neumann, F.; Thiesen, B.; et al. The effect of thermotherapy using magnetic nanoparticles on rat malignant glioma. *J. Neuro Oncol.* **2006**, *78*, 7–14. [[CrossRef](#)]
81. Veiseh, O.; Gunn, J.W.; Kievit, F.M.; Sun, C.; Fang, C.; Lee, J.S.H.; Zhang, M. Inhibition of tumor-cell invasion with chlorotoxin-bound superparamagnetic nanoparticles. *Small* **2009**, *5*, 256–264. [[CrossRef](#)] [[PubMed](#)]
82. Tan, J.; Sun, W.; Lu, L.; Xiao, Z.; Wei, H.; Shi, W.; Wang, Y.; Han, S.; Shuai, X. I6P7 peptide modified superparamagnetic iron oxide nanoparticles for magnetic resonance imaging detection of low-grade brain gliomas. *J. Mater. Chem. B* **2019**, *7*, 6139–6147. [[CrossRef](#)]
83. Wang, L.; Jang, G.; Ban, D.K.; Sant, V.; Seth, J.; Kazmi, S.; Patel, N.; Yang, Q.; Lee, J.; Janetanakit, W.; et al. Multifunctional stimuli responsive polymer-gated iron and gold-embedded silica nano golf balls: Nanoshuttles for targeted on-demand theranostics. *Bone Res.* **2017**, *5*. [[CrossRef](#)] [[PubMed](#)]
84. Ye, Q.; Zhou, F.; Liu, W. Bioinspired catecholic chemistry for surface modification. *Chem. Soc. Rev.* **2011**, *40*, 4244–4258. [[CrossRef](#)]
85. Yu, B.; Liu, J.; Liu, S.; Zhou, F. Pdop layer exhibiting zwitterionicity: A simple electrochemical interface for governing ion permeability. *Chem. Commun.* **2010**, *46*, 5900–5902. [[CrossRef](#)]
86. Richard, S.; Saric, A.; Boucher, M.; Slomianny, C.; Geffroy, F.; Mériaux, S.; Lalatonne, Y.; Motte, L. Anti-oxidative theranostic iron oxide nanoparticles towards brain tumors imaging and ROS production. *ACS Chem. Biol.* **2018**. [[CrossRef](#)]
87. Yang, X.; Hong, H.; Grailer, J.J.; Rowland, I.J.; Javadi, A.; Hurley, S.A.; Xiao, Y.; Yang, Y.; Zhang, Y.; Nickles, R.; et al. cRGD-functionalized, DOX-conjugated, and Cu-64-labeled superparamagnetic iron oxide nanoparticles for targeted anticancer drug delivery and PET/MR imaging. *Biomaterials* **2011**, *32*, 4151–4160. [[CrossRef](#)]
88. Laurent, S.; Forge, D.; Port, M.; Roch, A.; Robic, C.; Vander Elst, L.; Muller, R.N. Magnetic Iron Oxide Nanoparticles: Synthesis, stabilization, vectorization, physicochemical characterizations, and biological applications. *Chem. Rev.* **2008**, *108*, 2064–2110. [[CrossRef](#)] [[PubMed](#)]
89. Veiseh, O.; Kievit, F.M.; Gunn, J.W.; Ratner, B.D.; Zhang, M. A ligand-mediated nanovector for targeted gene delivery and transfection in cancer cells. *Biomaterials* **2009**, *30*, 649–657. [[CrossRef](#)] [[PubMed](#)]
90. Bai, Z.; Wei, J.; Yu, C.; Han, X.; Qin, X.; Zhang, C.; Liao, W.; Li, L.; Huang, W. Non-viral nanocarriers for intracellular delivery of microRNA therapeutics. *J. Mater. Chem. B* **2019**, *7*, 1209–1225. [[CrossRef](#)] [[PubMed](#)]
91. Molday, R.S.; Mackenzie, D. Immunospecific ferromagnetic iron-dextran reagents for the labeling and magnetic separation of cells. *J. Immunol. Methods* **1982**, *52*, 353–367. [[CrossRef](#)]
92. Wan, X.Y.; Song, Y.Q.; Song, N.J.; Li, J.H.; Yang, L.; Li, Y.; Tan, H. The preliminary study of immune superparamagnetic Iron Oxide Nanoparticles for the detection of lung cancer in magnetic resonance imaging. *Carbohydr. Res.* **2016**, *419*, 33–40. [[CrossRef](#)] [[PubMed](#)]
93. Lin, M.M.; Li, S.H.; Kim, H.H.; Kim, H.; Lee, H.B.; Muhammed, M.; Kim, D.K. Complete separation of magnetic nanoparticles via chemical cleavage of dextran by ethylenediamine for intracellular uptake. *J. Mater. Chem.* **2010**, *20*, 444–447. [[CrossRef](#)]



94. Tassa, C.; Shaw, S.Y.; Weissleder, R. Dextran-Coated Iron Oxide Nanoparticles: A Versatile Platform for Targeted Molecular Imaging, Molecular Diagnostics, and Therapy. *Acc. Chem. Res.* **2011**, *44*, 842–852. [[CrossRef](#)] [[PubMed](#)]
95. Chung, T.-H.; Hsu, S.-C.; Wu, S.-H.; Hsiao, J.-K.; Lin, C.-P.; Yao, M.; Huang, D.-M. Dextran-coated iron oxide nanoparticle-improved therapeutic effects of human mesenchymal stem cells in a mouse model of Parkinson's disease. *Nanoscale* **2018**, *10*, 2998–3007. [[CrossRef](#)]
96. Pisanic, T.R.; Blackwell, J.D.; Shubayev, V.I.; Finones, R.R.; Jin, S. Nanotoxicity of Iron Oxide Nanoparticle internalization in growing neurons. *Biomaterials* **2007**, *28*, 2572–2581. [[CrossRef](#)]
97. Katebi, S.; Esmaili, A.; Ghaedi, K.; Zarrabi, A. Superparamagnetic iron oxide nanoparticles combined with NGF and quercetin promote neuronal branching morphogenesis of PC12 cells. *Int. J. Nanomed.* **2019**, *14*, 2157–2169. [[CrossRef](#)]
98. Artursson, P.; Lindmark, T.; Davis, S.S.; Illum, L. Effect of chitosan on the permeability of monolayers of intestinal epithelial-cells (caco-2). *Pharm. Res.* **1994**, *11*, 1358–1361. [[CrossRef](#)]
99. Guo, L.L.; Chen, H.; He, N.Y.; Deng, Y. Effects of surface modifications on the physicochemical properties of iron oxide nanoparticles and their performance as anticancer drug carriers. *Chin. Chem. Lett.* **2018**, *29*, 1829–1833. [[CrossRef](#)]
100. Kim, E.H.; Lee, H.S.; Kwak, B.K.; Kim, B.K. Synthesis of ferrofluid with magnetic nanoparticles by sonochemical method for MRI contrast agent. *J. Magn. Magn. Mater.* **2005**, *289*, 328–330. [[CrossRef](#)]
101. Bhattarai, S.R.; Kim, S.Y.; Jang, K.Y.; Lee, K.C.; Yi, H.K.; Lee, D.Y.; Kim, H.Y.; Hwang, P.H. Laboratory formulated magnetic nanoparticles for enhancement of viral gene expression in suspension cell line. *J. Virol. Methods* **2008**, *147*, 213–218. [[CrossRef](#)]
102. Zinadini, S.; Zinatizadeh, A.A.; Rahimi, M.; Vatanpour, V.; Zangeneh, H.; Beygzadeh, M. Novel high flux antifouling nanofiltration membranes for dye removal containing carboxymethyl chitosan coated Fe<sub>3</sub>O<sub>4</sub> nanoparticles. *Desalination* **2014**, *349*, 145–154. [[CrossRef](#)]
103. Kamalzare, S.; Noormohammadi, Z.; Rahimi, P.; Atyabi, F.; Irani, S.; Tekie, F.S.M.; Mottaghtalab, F. Carboxymethyl dextran-trimethyl chitosan coated superparamagnetic iron oxide nanoparticles: An effective siRNA delivery system for HIV-1 Nef. *J. Cell. Physiol.* **2019**, *234*, 20554–20565. [[CrossRef](#)] [[PubMed](#)]
104. Barrow, M.; Taylor, A.; Nieves, D.J.; Bogart, L.K.; Mandal, P.; Collins, C.M.; Moore, L.R.; Chalmers, J.J.; Levy, R.; Williams, S.R.; et al. Tailoring the surface charge of dextran-based polymer coated SPIONs for modulated stem cell uptake and MRI contrast. *Biomater. Sci.* **2015**, *3*, 608–616. [[CrossRef](#)]
105. Wang, X.Q.; Chang, Y.Y.; Zhang, D.X.; Tian, B.M.; Yang, Y.; Wei, F. Transferrin-conjugated drug/dye-co-encapsulated magnetic nanocarriers for active-targeting fluorescent/magnetic resonance imaging and anti-tumor effects in human brain tumor cells. *RSC Adv.* **2016**, *6*, 105661–105675. [[CrossRef](#)]
106. Walia, S.; Sharma, S.; Kulurkar, P.M.; Patial, V.; Acharya, A. A bimodal molecular imaging probe based on chitosan encapsulated magneto-fluorescent nanocomposite offers biocompatibility, visualization of specific cancer cells in vitro and lung tissues in vivo. *Int. J. Pharm.* **2016**, *498*, 110–118. [[CrossRef](#)] [[PubMed](#)]
107. Veiseh, O.; Gunn, J.W.; Zhang, M. Design and fabrication of magnetic nanoparticles for targeted drug delivery and imaging. *Adv. Drug Deliv. Rev.* **2010**, *62*, 284–304. [[CrossRef](#)]
108. Roberts, M.J.; Bentley, M.D.; Harris, J.M. Chemistry for peptide and protein PEGylation. *Adv. Drug Deliv. Rev.* **2012**, *64*, 116–127. [[CrossRef](#)]
109. Zhang, Y.; Kohler, N.; Zhang, M.Q. Surface modification of superparamagnetic magnetite nanoparticles and their intracellular uptake. *Biomaterials* **2002**, *23*, 1553–1561. [[CrossRef](#)]
110. Meng, Q.; Hu, H.; Zhou, L.; Zhang, Y.; Yu, B.; Shen, Y.; Cong, H. Logical design and application of prodrug platforms. *Polym. Chem.* **2019**, *10*, 306–324. [[CrossRef](#)]
111. Lutz, J.-F.; Stiller, S.; Hoth, A.; Kaufner, L.; Pison, U.; Cartier, R. One-pot synthesis of PEGylated ultrasmall iron-oxide nanoparticles and their in vivo evaluation as magnetic resonance imaging contrast agents. *Biomacromolecules* **2006**, *7*, 3132–3138. [[CrossRef](#)] [[PubMed](#)]
112. Kohler, N.; Fryxell, G.E.; Zhang, M.Q. A bifunctional poly(ethylene glycol) silane immobilized on metallic oxide-based nanoparticles for conjugation with cell targeting agents. *J. Am. Chem. Soc.* **2004**, *126*, 7206–7211. [[CrossRef](#)] [[PubMed](#)]
113. Stephen, Z.R.; Gebhart, R.N.; Jeon, M.; Blair, A.A.; Ellenbogen, R.G.; Silber, J.R.; Zhang, M. pH-Sensitive O<sub>6</sub>-Benzylguanosine polymer modified magnetic nanoparticles for treatment of glioblastomas. *Bioconjugate Chem.* **2017**, *28*, 194–202. [[CrossRef](#)] [[PubMed](#)]

114. Kohler, N.; Sun, C.; Fichtenholtz, A.; Gunn, J.; Fang, C.; Zhang, M.Q. Methotrexate-immobilized poly(ethylene glycol) magnetic nanoparticles for MR imaging and drug delivery. *Small* **2006**, *2*, 785–792. [[CrossRef](#)]
115. Kievit, F.M.; Wang, F.Y.; Fang, C.; Mok, H.; Wang, K.; Silber, J.R.; Ellenbogen, R.G.; Zhang, M. Doxorubicin loaded iron oxide nanoparticles overcome multidrug resistance in cancer in vitro. *J. Control. Release* **2011**, *152*, 76–83. [[CrossRef](#)]
116. Norouzi, M.; Yathindranath, V.; Thliveris, J.A.; Miller, D.W. Salinomycin-loaded Iron Oxide Nanoparticles for glioblastoma therapy. *Nanomaterials* **2020**, *10*, 447. [[CrossRef](#)]
117. Chen, Z.; Lv, Z.; Sun, Y.; Chi, Z.; Qing, G. Recent advancements in polyethyleneimine-based materials and their biomedical, biotechnology, and biomaterial applications. *J. Mater. Chem. B* **2020**, *8*, 2951–2973. [[CrossRef](#)]
118. Yan, H.; Zhu, D.; Zhou, Z.; Liu, X.; Piao, Y.; Zhang, Z.; Liu, X.; Tang, J.; Shen, Y. Facile synthesis of semi-library of low charge density cationic polyesters from poly(alkylene maleate)s for efficient local gene delivery. *Biomaterials* **2018**, *178*, 559–569. [[CrossRef](#)]
119. Yang, J.; Liu, H.; Zhang, X. Design, preparation and application of nucleic acid delivery carriers. *Biotechnol. Adv.* **2014**, *32*, 804–817. [[CrossRef](#)]
120. Steitz, B.; Hofmann, H.; Kamau, S.W.; Hassa, P.O.; Hottiger, M.O.; von Rechenberg, B.; Hofmann-Antenbrink, M.; Petri-Fink, A. Characterization of PEI-coated superparamagnetic iron oxide nanoparticles for transfection: Size distribution, colloidal properties and DNA interaction. *J. Magn. Magn. Mater.* **2007**, *311*, 300–305. [[CrossRef](#)]
121. Chertok, B.; David, A.E.; Yang, V.C. Polyethyleneimine-modified iron oxide nanoparticles for brain tumor drug delivery using magnetic targeting and intra-carotid administration. *Biomaterials* **2010**, *31*, 6317–6324. [[CrossRef](#)] [[PubMed](#)]
122. Dai, F.; Du, M.; Liu, Y.; Liu, G.; Liu, Q.; Zhang, X. Folic acid-conjugated glucose and dextran coated iron oxide nanoparticles as MRI contrast agents for diagnosis and treatment response of rheumatoid arthritis. *J. Mater. Chem. B* **2014**, *2*, 2240–2247. [[CrossRef](#)] [[PubMed](#)]
123. Mok, H.; Veiseh, O.; Fang, C.; Kievit, F.M.; Wang, F.Y.; Park, J.O.; Zhang, M. pH-Sensitive siRNA nanovector for targeted gene silencing and cytotoxic effect in cancer cells. *Mol. Pharm.* **2010**, *7*, 1930–1939. [[CrossRef](#)] [[PubMed](#)]
124. Veiseh, O.; Kievit, F.M.; Fang, C.; Mu, N.; Jana, S.; Leung, M.C.; Mok, H.; Ellenbogen, R.G.; Park, J.O.; Zhang, M. Chlorotoxin bound magnetic nanovector tailored for cancer cell targeting, imaging, and siRNA delivery. *Biomaterials* **2010**, *31*, 8032–8042. [[CrossRef](#)] [[PubMed](#)]
125. Song, H.; Wang, C.; Zhan, H.; Yao, L.; Zhang, J.; Gao, R.; Tang, X.; Chong, T.; Liu, W.; Tang, Y. A high-loading drug delivery system based on magnetic nanomaterials modified by hyperbranched phenylboronic acid for tumor-targeting treatment with pH response. *Colloids Surf. B-Biointerfaces* **2019**, *182*. [[CrossRef](#)] [[PubMed](#)]
126. Huang, R.-Y.; Chiang, P.-H.; Hsiao, W.-C.; Chuang, C.-C.; Chang, C.-W. Redox-Sensitive Polymer/SPIO Nanocomplexes for Efficient Magnetofection and MR Imaging of Human Cancer Cells. *Langmuir* **2015**, *31*, 6523–6531. [[CrossRef](#)]
127. Li, Y.; Cheng, Q.; Jiang, Q.; Huang, Y.; Liu, H.; Zhao, Y.; Cao, W.; Ma, G.; Dai, F.; Liang, X.; et al. Enhanced endosomal/lysosomal escape by distearoyl phosphoethanolamine-polycarboxybetaine lipid for systemic delivery of siRNA. *J. Control. Release* **2014**, *176*, 104–114. [[CrossRef](#)]
128. Li, Y.; Li, Y.; Ji, W.; Lu, Z.; Liu, L.; Shi, Y.; Ma, G.; Zhang, X. Positively charged polyprodrug amphiphiles with enhanced drug loading and reactive oxygen species-responsive release ability for traceable synergistic therapy. *J. Am. Chem. Soc.* **2018**, *140*, 4164–4171. [[CrossRef](#)]
129. Zhang, R.; Li, Y.; Hu, B.; Lu, Z.; Zhang, J.; Zhang, X. Traceable nanoparticle delivery of small interfering rna and retinoic acid with temporally release ability to control neural stem cell differentiation for alzheimer's disease therapy. *Adv. Mater.* **2016**, *28*, 6345–6352. [[CrossRef](#)]
130. Martins, C.; Sousa, F.; Araujo, F.; Sarmiento, B. Functionalizing PLGA and PLGA derivatives for drug delivery and tissue regeneration applications. *Adv. Healthc. Mater.* **2018**, *7*, 24. [[CrossRef](#)]
131. Ganipineni, L.P.; Ucakar, B.; Joudiou, N.; Bianco, J.; Danhier, P.; Zhao, M.; Bastiancich, C.; Gallez, B.; Danhier, F.; Preat, V. Magnetic targeting of paclitaxel-loaded poly(lactic-co-glycolic acid)-based nanoparticles for the treatment of glioblastoma. *Int. J. Nanomed.* **2018**, *13*, 4509–4521. [[CrossRef](#)] [[PubMed](#)]
132. Soenen, S.J.; Vande Velde, G.; Ketkar-Atre, A.; Himmelreich, U.; De Cuyper, M. Magnetoliposomes as magnetic resonance imaging contrast agents. *Wiley Interdiscip. Rev. Nanomed. Nanobiotechnol.* **2011**, *3*, 197–211. [[CrossRef](#)]
133. Sawant, R.R.; Torchilin, V.P. Liposomes as 'smart' pharmaceutical nanocarriers. *Soft Matter* **2010**, *6*, 4026–4044. [[CrossRef](#)]

134. Ji, W.H.; Xiao, Z.B.; Liu, G.Y.; Zhang, X. Development and application of nano-flavor-drug carriers in neurodegenerative diseases. *Chin. Chem. Lett.* **2017**, *28*, 1829–1834. [[CrossRef](#)]
135. Maeda, H.; Wu, J.; Sawa, T.; Matsumura, Y.; Hori, K. Tumor vascular permeability and the EPR effect in macromolecular therapeutics: A review. *J. Control. Release* **2000**, *65*, 271–284. [[CrossRef](#)]
136. Li, Y.; Liu, R.; Yang, J.; Shi, Y.; Ma, G.; Zhang, Z.; Zhang, X. Enhanced retention and anti-tumor efficacy of liposomes by changing their cellular uptake and pharmacokinetics behavior. *Biomaterials* **2015**, *41*, 1–14. [[CrossRef](#)] [[PubMed](#)]
137. Mullis, A.S.; Schlichtmann, B.W.; Narasimhan, B.; Cademartiri, R.; Mallapragada, S.K. Ligand-cascading nano-delivery devices to enable multiscale targeting of anti-neurodegenerative therapeutics. *Biomed. Mater.* **2018**, *13*. [[CrossRef](#)] [[PubMed](#)]
138. Hu, B.; Dai, F.; Fan, Z.; Ma, G.; Tang, Q.; Zhang, X. Nanotheranostics: Congo Red/Rutin-MNPs with Enhanced Magnetic Resonance Imaging and H<sub>2</sub>O<sub>2</sub>-Responsive Therapy of Alzheimer's Disease in APPswe/PS1dE9 Transgenic Mice. *Adv. Mater.* **2015**, *27*, 5499–5505. [[CrossRef](#)] [[PubMed](#)]
139. Xu, H.-L.; Yang, J.-J.; Zhuge, D.-L.; Lin, M.-T.; Zhu, Q.-Y.; Jin, B.-H.; Tong, M.-Q.; Shen, B.-X.; Xiao, J.; Zhao, Y.-Z. Glioma-targeted delivery of a theranostic liposome integrated with quantum dots, superparamagnetic Iron Oxide, and cilengitide for dual-imaging guiding cancer surgery. *Adv. Healthc. Mater.* **2018**, *7*. [[CrossRef](#)]
140. Luchini, A.; Vitiello, G. Understanding the nano-bio interfaces: Lipid-coatings for inorganic nanoparticles as promising strategy for biomedical applications. *Front. Chem.* **2019**, *7*, 16. [[CrossRef](#)]
141. Gill, K.K.; Kaddoumi, A.; Nazzal, S. PEG-lipid micelles as drug carriers: Physicochemical attributes, formulation principles and biological implication. *J. Drug Target.* **2015**, *23*, 222–231. [[CrossRef](#)] [[PubMed](#)]
142. Wang, J.Q.; Hu, S.Q.; Mao, W.W.; Xiang, J.J.; Zhou, Z.X.; Liu, X.R.; Tang, J.B.; Shen, Y.Q. Assemblies of peptide-cytotoxin conjugates for tumor-homing chemotherapy. *Adv. Funct. Mater.* **2019**, *29*, 10.
143. Lukyanov, A.N.; Gao, Z.G.; Mazzola, L.; Torchilin, V.P. Polyethylene glycol-diacyl lipid micelles demonstrate increased accumulation in subcutaneous tumors in mice. *Pharm. Res.* **2002**, *19*, 1424–1429. [[CrossRef](#)] [[PubMed](#)]
144. Lu, Z.; Li, Y.; Shi, Y.; Li, Y.; Xiao, Z.; Zhang, X. Traceable nanoparticles with spatiotemporally controlled release ability for synergistic glioblastoma multiforme treatment. *Adv. Funct. Mater.* **2017**, *27*. [[CrossRef](#)]
145. Qiao, C.; Yang, J.; Shen, Q.; Liu, R.; Li, Y.; Shi, Y.; Chen, J.; Shen, Y.; Xiao, Z.; Weng, J.; et al. Traceable nanoparticles with dual targeting and ROS response for RNAi-Based immunochemotherapy of intracranial glioblastoma treatment. *Adv. Mater.* **2018**, *30*, e1705054. [[CrossRef](#)] [[PubMed](#)]
146. Gawande, M.B.; Monga, Y.; Zboril, R.; Sharma, R.K. Silica-decorated magnetic nanocomposites for catalytic applications. *Coord. Chem. Rev.* **2015**, *288*, 118–143. [[CrossRef](#)]
147. Chen, Y.J.; Tao, J.A.; Xiong, F.; Zhu, J.B.; Gu, N.; Zhang, Y.H.; Ding, Y.; Ge, L.A. Synthesis, self-assembly, and characterization of PEG-coated iron oxide nanoparticles as potential MRI contrast agent. *Drug Dev. Ind. Pharm.* **2010**, *36*, 1235–1244.
148. Hu, Y.; Zhou, Y.; Zhao, N.; Liu, F.; Xu, F.-J. Multifunctional pDNA-Conjugated polycationic Au Nanorod-Coated Fe<sub>3</sub>O<sub>4</sub> hierarchical nanocomposites for trimodal imaging and combined photothermal/gene therapy. *Small* **2016**, *12*, 2459–2468. [[CrossRef](#)]
149. Yong, C.; Chen, X.; Xiang, Q.; Li, Q.; Xing, X. Recyclable magnetite-silver heterodimer nanocomposites with durable antibacterial performance. *Bioact. Mater.* **2018**, *3*, 80–86. [[CrossRef](#)]
150. Zhao, S.; Yu, X.; Qian, Y.; Chen, W.; Shen, J. Multifunctional magnetic iron oxide nanoparticles: An advanced platform for cancer theranostics. *Theranostics* **2020**, *10*, 6278–6309. [[CrossRef](#)]
151. Zhou, J.; Atsina, K.-B.; Himes, B.T.; Strohhahn, G.W.; Saltzman, W.M. Novel delivery strategies for glioblastoma. *Cancer J.* **2012**, *18*, 89–99. [[CrossRef](#)]
152. Mahmoudi, M.; Simchi, A.; Imani, M.; Haefeli, U.O. Superparamagnetic Iron Oxide Nanoparticles with rigid cross-linked polyethylene glycol fumarate coating for application in imaging and drug delivery. *J. Phys. Chem. C* **2009**, *113*, 8124–8131. [[CrossRef](#)]
153. Mahmoudi, M.; Sant, S.; Wang, B.; Laurent, S.; Sen, T. Superparamagnetic iron oxide nanoparticles (SPIONs): Development, surface modification and applications in chemotherapy. *Adv. Drug Deliv. Rev.* **2011**, *63*, 24–46. [[CrossRef](#)] [[PubMed](#)]

